MATHEMATICS OF COMPUTATION
Volume 88, Number 317, May 2019, Pages 1155–1188
https://doi.org/10.1090/mcom/3366
Article electronically published on July 6, 2018

SPECTRAL ANALYSIS AND SPECTRAL SYMBOL FOR THE 2D CURL-CURL (STABILIZED) OPERATOR WITH APPLICATIONS TO THE RELATED ITERATIVE SOLUTIONS

MARIAROSA MAZZA, AHMED RATNANI, AND STEFANO SERRA-CAPIZZANO

Abstract. In this paper, we study structural and spectral features of linear systems of equations arising from Galerkin approximations of $H(\mathrm{curl})$ elliptic variational problems, based on the Isogeometric Analysis (IgA) approach. Such problems arise in Time Harmonic Maxwell and Magnetostatic problems, as well in the preconditioning of MagnetoHydroDynamics equations, and lead to large linear systems, with different and severe sources of ill-conditioning.

First, we consider a compatible B-splines discretization based on a discrete de Rham sequence and we study the structure of the resulting matrices $\mathcal{A}_{\boldsymbol{n}}$. It turns out that $\mathcal{A}_{\boldsymbol{n}}$ shows a two-by-two pattern and is a principal submatrix of a two-by-two block matrix, where each block is two-level banded, almost Toeplitz, and where the bandwidths grow linearly with the degree of the B-splines.

Looking at the coefficients in detail and making use of the theory of the Generalized Locally Toeplitz (GLT) sequences, we identify the symbol of each of these blocks, that is, a function describing asymptotically, i.e., for $\boldsymbol{n}$ large enough, the spectrum of each block. From this spectral knowledge and thanks to some new spectral tools we retrieve the symbol of $\{\mathcal{A}_{\boldsymbol{n}}\}_{\boldsymbol{n}}$ which as expected is a two-by-two matrix-valued bivariate trigonometric polynomial. In particular, there is a nice elegant connection with the continuous operator, which has an infinite dimensional kernel, and in fact the symbol is a dyad having one eigenvalue like the one of the IgA Laplacian, and one identically zero eigenvalue; as a consequence, we prove that one half of the spectrum of $\mathcal{A}_{\boldsymbol{n}}$, for $\boldsymbol{n}$ large enough, is very close to zero and this represents the discrete counterpart of the infinite dimensional kernel of the continuous operator. From the latter information, showing that the considered problem has an ill-posed nature, we are able to give a detailed spectral analysis of the matrices $\mathcal{A}_{\boldsymbol{n}}$ and of the corresponding zero-order term stabilized matrices, which is fully confirmed by several numerical evidences.

Finally, by taking into consideration the GLT theory and making use of the spectral results, we furnish indications on the convergence features of known iterative solvers and we suggest a further stabilization technique and proper iterative procedures for the numerical solution of the involved linear systems.

1. Introduction

In many physics and engineering applications [3], the numerical discretization of electromagnetic problems and of the Maxwell equations is of critical importance.

Received by the editor April 14, 2017, and, in revised form, November 8, 2017, and February 11, 2018.

2010 *Mathematics Subject Classification.* Primary 15A18, 15B05, 41A15, 15A69, 35Q61.

Key words and phrases. Maxwell equations, compatible B-spline discretization, spectral distribution and spectral symbol, GLT matrix-sequence.

The work of the first and third authors was partly supported by GNCS-INDAM (Italy).

In real applications, for example, the Full-Wave problem with high wave numbers, the numerical simulation of such problems leads to huge sparse and ill-conditioned matrices and therefore the use of direct solvers is not possible. Iterative solvers are then the only possible choice, but suffer from ill-conditioning, where the latter is either caused by some physical parameters or by the used numerical method or by a combination of the two components. Furthermore, the need of robust and optimal *fast* solvers is motivated by the large-scale simulation codes and the architecture of modern super-computers. Such solvers have been extensively studied in the last two decades for standard discretizations [14, 15, 17, 18]. However, the spectral behavior of the resulting matrices is very involved and not favorable, so that this affected the design of fast and robust iterative solvers. In this direction, a valid alternative is represented by the Isogeometric Analysis (IgA); in fact, since its introduction [16], the IgA has proven to be a promising approach and, as for the Nodal Finite Elements case, it provides a discrete de Rham sequence [2]. However, by allowing the use of more regular basis functions, IgA-based matrices offer more favorable (spectral) properties compared to the case of Nodal Finite Elements methods (see the discussion on page 34 in [5] and the analysis of the spectral symbol for Finite Elements in [10]). In the case of maximum regularity, it turns out that we are able to describe easily the spectrum of the discrete operators, thanks to the Generalized Locally Toeplitz (GLT) theory [7–9, 25]. Moreover, IgA discretization can provide structured matrices and are then well adapted for the architecture of modern super-computers. Unfortunately, IgA is still a young topic and all the known results and developed methods for the standard discretizations are not yet available.

In this work, we are interested in the spectral study and analysis of the sequence of matrices corresponding to a compatible B-splines discretization of the following variational problem:

$$\boldsymbol{u} \in H(\mathrm{curl}, \Omega): \quad (\nabla \times \boldsymbol{u}, \nabla \times \boldsymbol{v}) + \mu\,(\boldsymbol{u}, \boldsymbol{v}) = (\boldsymbol{f}, \boldsymbol{v}), \quad \forall \boldsymbol{v} \in H(\mathrm{curl}, \Omega), \tag{1.1}$$

where $\boldsymbol{f}$ is a vector field in $(L^2(\Omega))^2$, $\mu \geq 0$, and

$$H(\mathrm{curl}, \Omega) := \{\boldsymbol{u} \in (L^2(\Omega))^2 \text{ s.t. } \nabla \times \boldsymbol{u} \in L^2(\Omega)\}.$$

It is worth noticing that variational problems of the form (1.1) arise in different applications such as Time Harmonic Maxwell equation and Magnetostatic problems (described by $\mu = 0$), as well as Time Domain Maxwell equations and Magneto-HydroDynamics problems, when using an implicit time stepping.

We focus our attention on a IgA discretization of problem (1.1), where we restrict the study to a 2D problem with $\Omega = [0, 1]^2$, in which case, the *curl* operator has the explicit expression $\nabla \times \boldsymbol{u} = \partial_x u^2 - \partial_y u^1$ for any $\boldsymbol{u} = [u^1(x, y), u^2(x, y)]^T$. Our first aim is to spectrally analyze the sequence of the resulting coefficient matrices and then to use such spectral information to suggest proper stabilizations and finally suitable iterative solvers for the corresponding linear systems.

First of all, the unstabilized matrix $\mathcal{A}_{\boldsymbol{n}}$ shows a two-by-two block structure and is a principal submatrix of a two-by-two block matrix, where each block is two-level banded, almost Toeplitz (i.e., Toeplitz up to small rank corrections), and where the bandwidths grow linearly with the degree of the B-splines.

After a careful study of the coefficients and making use of the theory of GLT sequences, we show that the four sequences containing these four Toeplitz-like blocks are all GLT sequences and we identify the symbol. According to Weyl, the symbol of a sequence of Hermitian (or quasi-Hermitian) matrices is a function describing

asymptotically, i.e., for $\boldsymbol{n}$ large enough, the spectrum of the $\boldsymbol{n}$th matrix. From this knowledge and as a consequence of some new spectral tools we recover the symbol of $\{\mathcal{A}_{\boldsymbol{n}}\}_{\boldsymbol{n}}$ which as expected is a two-by-two matrix-valued bivariate trigonometric polynomial. We show a nice and elegant connection between the discrete structures and the continuous operator, which has an infinite dimensional kernel. In fact the symbol of the discrete structures is a dyad having one eigenvalue like the one of the IgA Laplacian, and one identically zero eigenvalue; as a consequence, we prove that one half of the spectrum of $\mathcal{A}_{\boldsymbol{n}}$, for $\boldsymbol{n}$ large enough, is very close to zero and this represents the discrete counterpart of the infinite dimensional kernel of the continuous operator. Starting from these findings, we are able to furnish a detailed spectral analysis of the matrices $\mathcal{A}_{\boldsymbol{n}}$, which are fully confirmed by several numerical evidences. In particular, the fact that half of the spectrum is virtually zero shows that the discrete problem is not only highly ill-conditioned, but in fact it is related to an ill-posed problem and hence proper stabilization (or regularization) processes [6] have to be taken into account. Hence, by exploiting the spectral results, two stabilization techniques (of zero-order-type as in (1.1) and of divergence-type as in Subsection 4.5) are proposed. For such stabilized problems, we give indications on the convergence features of known iterative solvers and we suggest ad hoc iterative procedures for the numerical solution of the considered linear systems. Such a discussion is accompanied by a selection of numerical tests which are presented and critically discussed.

The overview of the paper is as follows. In Section 2 we give notations, definitions, and preliminary results. Section 3 is devoted to the IgA approximation of the variational problem reported in (1.1), by using B-splines, while in Section 4 we perform a detailed spectral analysis of the resulting matrices, by also providing new matrix-theoretic tools and by discussing few numerical tests, including algorithmic proposals (in Subsection 4.5) fully developed in [19]. Finally, in Section 5 we draw conclusions.

2. Notation and preliminaries

In this section we will introduce some preliminary approximation and spectral tools used throughout this paper. In detail, in Subsection 2.1 we will recall the definition of (cardinal) B-spline together with some relevant properties. Subsections 2.2 and 2.3 are devoted to spectral notions of multilevel block Toeplitz matrices and of GLT matrix-sequences, respectively. We will end this section collecting some spectral results on the matrices involved in the IgA discretization of 1D elliptic problems (Subsection 2.4), which will be widely used in the IgA discretization of the curl-curl problem discussed in Section 3.

2.1. B-splines and cardinal B-splines.

For $p, n \geq 1$ consider the uniform knot sequence

$$t_1 = \cdots = t_{p+1} = 0 < t_{p+2} < \cdots < t_{p+n} < 1 = t_{p+n+1} = \cdots = t_{2p+n+1}, \tag{2.1}$$

where

$$t_{i+p+1} = \frac{i}{n}, \quad i = 0, \ldots, n.$$

Definition 2.1. The B-splines of degree p on the knots sequence (2.1) are denoted by

$$N_i^p : [0,1] \to \mathbb{R}, \quad i = 1, \dots, n+p,$$

and are recursively defined as follows: for $1 \le i \le n+2p$,

$$N_i^0(t) = \chi_{[t_i, t_{i+1})}, \quad t \in [0,1];$$

for $1 \le k \le p$ and $1 \le i \le n+2p-k$,

$$N_i^k(t) = \frac{t - t_i}{t_{i+k} - t_i} N_i^{k-1}(t) + \frac{t_{i+k+1} - t}{t_{i+k+1} - t_{i+1}} N_{i+1}^{k-1}(t), \quad t \in [0,1],$$

where we assume a fraction with zero denominator to be zero.

It is well known that the functions in $\left\{N_1^p, \dots, N_{n+p}^p\right\}$ form a basis for the spline space of degree p. Moreover, the B-splines possess the following properties:

a1) Local support property:

$$\operatorname{supp}(N_i^p) = [t_i, t_{i+p+1}], \quad i = 1, \dots, n+p,$$

a2) Vanishing at the boundary:

$$N_i^p(0) = N_i^p(1) = 0, \quad i = 2, \dots, n+p-1,$$

a3) Nonnegative partition of unity:

$$N_i^p(t) \ge 0, \quad t \in [0,1], \quad i = 1, \dots, n+p,$$

$$\sum_{i=1}^{n+p} N_i^p(t) = 1, \quad t \in [0,1].$$

Now, we turn to the definition of cardinal B-splines.

Definition 2.2. A cardinal B-spline of zero degree, denoted by ϕ_0, is the characteristic function over the interval $[0,1)$, i.e.,

$$\phi_0(t) := \begin{cases} 1, & t \in [0,1), \\ 0, & \text{otherwise.} \end{cases}$$

A cardinal B-Spline of degree q, $q \in \mathbb{N}$, denoted by ϕ_q, is defined by convolution as

$$\phi_q(t) = (\phi_{q-1} * \phi_0)(t) = \int_{\mathbb{R}} \phi_{q-1}(t-s)\phi_0(s)\, ds.$$

A cardinal B-Spline of degree q has the following properties:

b1) Local support property:

$$\operatorname{supp}(\phi_q) = [0, q+1];$$

b2) Regularity: $\phi_q \in \mathcal{C}^{q-1}$;

b3) Derivative expression: $\forall t \in [0, q+1]$ and $q \ge 1$, we have

$$\phi_q'(t) = \phi_{q-1}(t) - \phi_{q-1}(t-1);$$

b4) Recursive definition: $\forall t \in [0, q+1]$ and $q \ge 1$, we have

$$\phi_q(t) = \frac{t}{q}\phi_{q-1}(t) + \frac{q+1-t}{q}\phi_{q-1}(t-1);$$

b5) Symmetry: ϕ_q is symmetric on the interval $[0, q+1]$, i.e.,

$$\phi_q(t) = \phi_q(q+1-t), \quad \forall t \in [0, q+1];$$

b6) Inner product: for $\tau \in \mathbb{R}$, $q_1, q_2, r_1, r_2 \geq 0$,

$$\int_{\mathbb{R}} \phi_{q_1}^{(r_1)}(t)\phi_{q_2}^{(r_2)}(t+\tau)\, dt = (-1)^{r_1}\phi_{q_1+q_2+1}^{(r_1+r_2)}(q_1+1+\tau) = (-1)^{r_2}\phi_{q_1+q_2+1}^{(r_1+r_2)}(q_2+1-\tau).$$

Cardinal B-splines are of interest since the so-called central basis functions N_i^p, $i = p+1, \ldots, n$, are the uniformly shifted and scaled versions of the cardinal B-splines ϕ_p. More precisely, we have

$$N_i^p(t) = \phi_p(nt - i + p + 1), \quad i = p+1, \ldots, n, \tag{2.2}$$

$$\left(N_i^p(t)\right)' = n\phi_p'(nt - i + p + 1), \quad i = p+1, \ldots, n. \tag{2.3}$$

We end this subsection by introducing the tensor product B-splines.

Definition 2.3. For any pair of d-indices $\boldsymbol{n} = (n_1, n_2, \ldots, n_d)$ and $\boldsymbol{p} = (p_1, p_2, \ldots, p_d)$, let us define the tensor product B-splines as follows:

$$N_{\boldsymbol{i}}^{\boldsymbol{p}} : [0,1]^d \to \mathbb{R}, \quad N_{\boldsymbol{i}}^{\boldsymbol{p}}(\boldsymbol{t}) = \prod_{j=1}^{d} N_{i_j}^{p_j}(t_j), \quad \boldsymbol{i} = \boldsymbol{1}, \ldots, \boldsymbol{n} + \boldsymbol{p},$$

where $\boldsymbol{t} = (t_1, \ldots, t_d) \in [0,1]^d$, $\boldsymbol{1} = (1, \ldots, 1) \in \mathbb{N}^d$, $\boldsymbol{i} = (i_1, \ldots, i_d) \in \mathbb{N}^d$.

In the remaining, our attention will be focused on the 2D tensor-product B-spline space

$$S^{p_1,p_2} := \operatorname{span}\left\{N_{i_1}^{p_1}(t_1)N_{i_2}^{p_2}(t_2)\right\}_{i_1,i_2}, \quad \begin{matrix} i_1 = 1, \ldots, n_1 + p_1, \\ i_2 = 1, \ldots, n_2 + p_2. \end{matrix} \tag{2.4}$$

2.2. **Unilevel and multilevel Toeplitz matrix-sequences.**

Definition 2.4. A (unilevel) Toeplitz matrix is a real/complex valued $n \times n$ matrix $T_n = [t_{ij}]_{i,j=1}^n$, where $t_{ij} = t_{i-j}$, i.e.,

$$T_n = \begin{bmatrix} t_0 & t_{-1} & t_{-2} & \ldots & t_{-(n-1)} \\ t_1 & t_0 & t_{-1} & \ldots & \\ t_2 & t_1 & t_0 & \ldots & \vdots \\ \vdots & & & \ddots & \\ t_{n-1} & \ldots & & \ldots & t_0 \end{bmatrix}.$$

For any function $f \in L^1([-\pi, \pi])$, the Fourier coefficients are defined as

$$\hat{f}_j = \frac{1}{2\pi}\int_{-\pi}^{\pi} f(\theta)e^{-\mathbf{i}j\theta}\, d\theta, \qquad \mathbf{i}^2 = -1,$$

where the sequence $\{\hat{f}_j\}_j$ determines uniquely the function f and vice versa. Therefore, the function f, if it exists, is also uniquely determined by the sequence of the Toeplitz matrices $\{T_n(f)\}_n$ with

$$T_n(f) = \left[\hat{f}_{i-j}\right]_{i,j=1}^n.$$

When $f \in L^1([-\pi, \pi]^d)$, the associated sequence is made of the so-called *multilevel Toeplitz matrices*, that is, matrices which "at each level" are Toeplitz matrices. For example, a 2-level matrix is a block Toeplitz whose blocks are still Toeplitz.

A more general definition of Toeplitz sequences associated to a function is obtained when f is a matrix-valued function $f : [-\pi,\pi]^d \to \mathbb{C}^{s\times s}$ such that all its components $f_{ij} : [-\pi,\pi]^d \to \mathbb{C},\ i,j = 1,\dots,s$, belong to $L^1([-\pi,\pi]^d)$. In this case the associated sequence is made of the so-called *multilevel block Toeplitz matrices*, that is, multilevel Toeplitz matrices whose entries "at the last level" are $s \times s$ matrices themselves.

Let $\boldsymbol{n} := (n_1,\dots,n_d)$ be a multi-index in $\mathbb{N}^d$ and set $N(\boldsymbol{n}) := \prod_{i=1}^d n_i$. The formal definition of d-level block Toeplitz sequence associated to f is the following.

Definition 2.5. Let $f : [-\pi,\pi]^d \to \mathbb{C}^{s\times s}$ such that $f_{ij} \in L^1([-\pi,\pi]^d)$, $i,j = 1,\dots,s$, and let $\hat{f}_{\boldsymbol{j}}$ be its Fourier coefficients

$$\hat{f}_{\boldsymbol{j}} := \frac{1}{(2\pi)^d}\int_{[-\pi,\pi]^d} f(\boldsymbol{\theta})\mathrm{e}^{-\mathbf{i}\langle \boldsymbol{j},\boldsymbol{\theta}\rangle}\, d\boldsymbol{\theta} \in \mathbb{C}^{s\times s}, \tag{2.5}$$

where $\boldsymbol{j} = (j_1,\dots,j_d) \in \mathbb{Z}^d$, $\boldsymbol{\theta} = (\theta_1,\dots,\theta_d) \in [-\pi,\pi]^d$, $\langle \boldsymbol{j},\boldsymbol{\theta}\rangle = \sum_{r=1}^d j_r\theta_r$ and the integrals in (2.5) are computed componentwise. Then, the $\boldsymbol{n}$th Toeplitz matrix associated with f is the matrix of order $sN(\boldsymbol{n})$ given by

$$T_{\boldsymbol{n}}(f) = \left[\hat{f}_{\boldsymbol{i}-\boldsymbol{j}}\right]_{\boldsymbol{i},\boldsymbol{j}=\boldsymbol{1}}^{\boldsymbol{n}} = \sum_{|j_1|<n_1} \cdots \sum_{|j_d|<n_d} \left[J_{n_1}^{(j_1)} \otimes \cdots \otimes J_{n_d}^{(j_d)}\right] \otimes \hat{f}_{\boldsymbol{j}},$$

where $\boldsymbol{1} = (1,\dots,1) \in \mathbb{N}^d, \boldsymbol{i} = (i_1,\dots,i_d) \in \mathbb{N}^d, \boldsymbol{j} = (j_1,\dots,j_d) \in \mathbb{N}^d$ and $\otimes$ denotes the (Kronecker) tensor product of matrices. The term $J_m^{(l)}$ is the matrix of order m whose (i,j) entry equals 1 if $i-j=l$ and zero otherwise. The set $\{T_{\boldsymbol{n}}(f)\}_{\boldsymbol{n}}$ is called the *family of d-level block Toeplitz matrices generated by f*, that in turn is referred to as the *generating function* of $\{T_{\boldsymbol{n}}(f)\}_{\boldsymbol{n}}$.

In the next subsection, in Theorem 2.9 we will see that if f is a Hermitian matrix-valued function, then $(f,[-\pi,\pi]^d)$ is also the (spectral) symbol of $\{T_{\boldsymbol{n}}(f)\}_{\boldsymbol{n}}$, in the sense of Definition 2.6 and with f being the generating function.

2.3. **Summary of the theory of GLT sequences.** In the sequel, we recall the basic properties of the Generalized Locally Toeplitz sequences. More details can be found in the pioneering work [26] by Tilli and in the recent book [8], dealing with the spectrum of approximated one-dimensional differential operators, while in [9,24,25] a more general GLT theory is developed, with applications to the approximation of partial differential equations. As described in [24,25], a GLT sequence $\{A_{\boldsymbol{n}}\}_{\boldsymbol{n}}$ is a sequence of matrices of increasing size. Before listing some crucial properties of the GLT sequences, we need to introduce the definition of spectral distribution in the sense of the eigenvalues and of the singular values for a generic matrix-sequence $\{A_{\boldsymbol{n}}\}_{\boldsymbol{n}}$.

Definition 2.6. Let $f : G \to \mathbb{C}^{s\times s}$ be a measurable function, defined on a measurable set $G \subset \mathbb{R}^l$ with $l \geq 1$, $0 < m_l(G) < \infty$, where m_l is the Lebesgue measure. Let $\mathcal{C}_0(\mathbb{K})$ be the set of continuous functions with compact support over $\mathbb{K} \in \{\mathbb{C},\mathbb{R}_0^+\}$ and let $\{A_{\boldsymbol{n}}\}_{\boldsymbol{n}}$ be a sequence of matrices with $\dim(A_{\boldsymbol{n}}) = d_{\boldsymbol{n}}$ and $d_{\boldsymbol{n}} \to \infty$, $\boldsymbol{n} := (n_1,\dots,n_d)$, as $\boldsymbol{n} \to \infty$, i.e., $n_j \to \infty$, $j = 1,\dots,d$.

- $\{A_{\boldsymbol{n}}\}_{\boldsymbol{n}}$ is *distributed as the pair (f,G) in the sense of the eigenvalues,* that is,

$$\{A_{\boldsymbol{n}}\}_{\boldsymbol{n}} \sim_\lambda (f,G),$$

if the following limit relation holds for all $F \in \mathcal{C}_0(\mathbb{C})$:

$$\lim_{\boldsymbol{n}\to\infty} \frac{1}{d_{\boldsymbol{n}}} \sum_{j=1}^{d_{\boldsymbol{n}}} F(\lambda_j(A_{\boldsymbol{n}})) = \frac{1}{m_l(G)} \int_G \frac{\sum_{i=1}^{s} F(\lambda_i(f(\boldsymbol{t})))}{s} d\boldsymbol{t}, \tag{2.6}$$

where $\lambda_j(A_{\boldsymbol{n}})$, $j = 1, \ldots, d_{\boldsymbol{n}}$ are the eigenvalues of $A_{\boldsymbol{n}}$ and $\lambda_i(f)$, $i = 1, \ldots, s$ are the eigenvalues of f. In this case, we say that f is the *(spectral) symbol* of the matrix-sequence $\{A_{\boldsymbol{n}}\}_{\boldsymbol{n}}$.

- $\{A_{\boldsymbol{n}}\}_{\boldsymbol{n}}$ is *distributed as the pair* (f, G) *in the sense of the singular values,* that is,

$$\{A_{\boldsymbol{n}}\}_{\boldsymbol{n}} \sim_\sigma (f, G),$$

if the following limit relation holds for all $F \in \mathcal{C}_0(\mathbb{R}_0^+)$:

$$\lim_{\boldsymbol{n}\to\infty} \frac{1}{d_{\boldsymbol{n}}} \sum_{j=1}^{d_{\boldsymbol{n}}} F(\sigma_j(A_{\boldsymbol{n}})) = \frac{1}{m_l(G)} \int_G \frac{\sum_{i=1}^{s} F(\sigma_i(f(\boldsymbol{t})))}{s} d\boldsymbol{t}, \tag{2.7}$$

where $\sigma_j(A_{\boldsymbol{n}})$, $j = 1, \ldots, d_{\boldsymbol{n}}$ are the singular values of $A_{\boldsymbol{n}}$ and $\sigma_i(f)$, $i = 1, \ldots, s$ are the singular values of f. In this case, we say that f is the *singular value symbol* of the matrix-sequence $\{A_{\boldsymbol{n}}\}_{\boldsymbol{n}}$.

Remark 2.7. If f is smooth enough, an informal interpretation of the limit relation (2.6) (resp. (2.7)) is that when the matrix-size of $A_{\boldsymbol{n}}$ is sufficiently large, then $d_{\boldsymbol{n}}/s$ eigenvalues (resp. singular values) of $A_{\boldsymbol{n}}$ can be approximated by a sampling of $\lambda_1(f)$ (resp. $\sigma_1(f)$) on a uniform equispaced grid of the domain G, and so on until the last $d_{\boldsymbol{n}}/s$ eigenvalues (resp. singular values) that can be approximated by an equispaced sampling of $\lambda_s(f)$ (resp. $\sigma_s(f)$) in the domain.

In the following, we recall two well-known results on the spectral distribution of Toeplitz sequences. If f is a real-valued function, the following theorem due to Szegö holds.

Theorem 2.8 ([13])**.** *Let $f \in L^1([-\pi,\pi]^d)$ be a real-valued function. Then, $\{T_{\boldsymbol{n}}(f)\}_{\boldsymbol{n}} \sim_\lambda (f, [-\pi,\pi]^d)$.*

In the case where f is a Hermitian matrix-valued function, the previous theorem can be extended as follows.

Theorem 2.9 ([27])**.** *Let $f : [-\pi,\pi]^d \to \mathbb{C}^{s\times s}$ be a Hermitian matrix-valued function. Then, $\{T_{\boldsymbol{n}}(f)\}_{\boldsymbol{n}} \sim_\lambda (f, [-\pi,\pi]^d)$.*

We are now ready to provide more details on the GLT sequences. Each GLT sequence is *associated* to a *complex-valued* Lebesgue-measurable function κ, which is known as the *symbol* of the sequence $\{A_{\boldsymbol{n}}\}_{\boldsymbol{n}}$. In this case, we write $\{A_{\boldsymbol{n}}\}_{\boldsymbol{n}} \sim_{\text{GLT}} \kappa$. The domain of definition G of the symbol is taken as $[0,1]^d \times [-\pi,\pi]^d$ while a point in G is denoted by $(\boldsymbol{x}, \boldsymbol{\theta})$, where $\boldsymbol{x} = (x_1, \ldots, x_d)$ are the *physical variables* and $\boldsymbol{\theta} = (\theta_1, \ldots, \theta_d)$ are the *Fourier variables*.

We recall the following properties of a GLT sequence $\{A_{\boldsymbol{n}}\}_{\boldsymbol{n}}$:

GLT1. Let $\{A_{\boldsymbol{n}}\}_{\boldsymbol{n}} \sim_{\text{GLT}} \kappa$ with $\kappa : G \to \mathbb{C}$, $G = [0,1]^d \times [-\pi,\pi]^d$, then $\{A_{\boldsymbol{n}}\}_{\boldsymbol{n}} \sim_\sigma (\kappa, G)$. If the matrices $A_{\boldsymbol{n}}$ are definitely Hermitian, that is, $A_{\boldsymbol{n}} - A_{\boldsymbol{n}}^H$ is "small enough" (see Theorem 3.4 in [12]), then it holds also that $\{A_{\boldsymbol{n}}\}_{\boldsymbol{n}} \sim_\lambda (\kappa, G)$.

GLT2. The set of GLT sequences form a $*$-algebra, i.e., it is closed under linear combinations, products, inversion, conjugation: hence, the sequence obtained via algebraic operations on a finite set of input GLT sequences is still a GLT sequence and its symbol is obtained by following the same algebraic manipulations on the corresponding symbols of the input GLT sequences. In formulae, let $\{A_{\boldsymbol{n}}\}_{\boldsymbol{n}} \sim_{\text{GLT}} \kappa_1$ and $\{B_{\boldsymbol{n}}\}_{\boldsymbol{n}} \sim_{\text{GLT}} \kappa_2$, then
- $\{\alpha A_{\boldsymbol{n}} + \beta B_{\boldsymbol{n}}\}_{\boldsymbol{n}} \sim_{\text{GLT}} \alpha\kappa_1 + \beta\kappa_2, \quad \alpha, \beta \in \mathbb{C}$;
- $\{A_{\boldsymbol{n}} B_{\boldsymbol{n}}\}_{\boldsymbol{n}} \sim_{\text{GLT}} \kappa_1\kappa_2$;
- if κ_1 vanishes, at most, in a set of zero Lebesgue measure, then $\{A_{\boldsymbol{n}}^{-1}\}_{\boldsymbol{n}} \sim_{\text{GLT}} \kappa_1^{-1}$;
- $\{A_{\boldsymbol{n}}^H\}_{\boldsymbol{n}} \sim_{\text{GLT}} \bar{\kappa_1}$.

GLT3. Any sequence of Toeplitz matrices $\{T_{\boldsymbol{n}}(f)\}_{\boldsymbol{n}}$ generated by a function $f \in L^1([-\pi,\pi]^d)$ is a GLT sequence with symbol $\kappa(\boldsymbol{x},\boldsymbol{\theta}) = f(\boldsymbol{\theta})$.

GLT4. Any sequence of diagonal matrices $\{D_{\boldsymbol{n}}(a)\}_{\boldsymbol{n}}$ whose diagonal is made of the evaluations of a Riemann-integrable function $a : [0,1]^d \to \mathbb{C}$ over a uniform grid is a GLT sequence with symbol $\kappa(\boldsymbol{x},\boldsymbol{\theta}) = a(\boldsymbol{x})$.

GLT5. Every sequence which is distributed as the constant zero in the singular value sense is a GLT sequence with symbol 0 and vice versa, i.e., $\{A_{\boldsymbol{n}}\}_{\boldsymbol{n}} \sim_\sigma 0 \iff \{A_{\boldsymbol{n}}\}_{\boldsymbol{n}} \sim_{\text{GLT}} 0$.

We end this subsection introducing the notion of zero-distributed matrix-sequences and giving a characterization for them.

Definition 2.10. Let $\{A_{\boldsymbol{n}}\}_{\boldsymbol{n}}$ be a sequence of matrices with $\dim(A_{\boldsymbol{n}}) = d_{\boldsymbol{n}}$ and $d_{\boldsymbol{n}} \to \infty$ as $\boldsymbol{n} \to \infty$. We say that $\{A_{\boldsymbol{n}}\}_{\boldsymbol{n}}$ is a *zero-distributed matrix-sequence* if $\{A_{\boldsymbol{n}}\}_{\boldsymbol{n}} \sim_\sigma 0$.

Theorem 2.11 ([8, Theorem 3.2])**.** *The matrix-sequence $\{A_{\boldsymbol{n}}\}_{\boldsymbol{n}}$ is zero-distributed if and only if for all $\boldsymbol{n} \in \mathbb{N}^d$,*

$$A_{\boldsymbol{n}} = R_{\boldsymbol{n}} + N_{\boldsymbol{n}},$$

where

$$\lim_{\boldsymbol{n}\to\infty} \frac{\operatorname{rank}(R_{\boldsymbol{n}})}{d_{\boldsymbol{n}}} = \lim_{\boldsymbol{n}\to\infty} \|N_{\boldsymbol{n}}\| = 0.$$

Here $\|\cdot\|$ is the spectral norm.

2.4. **IgA mass and stiffness matrices.** In the context of IgA discretization of elliptic problems, we often deal with the following mass and stiffness matrices

$$M_n^p = \left[\int_0^1 N_{i_1}^p(t)\ N_{j_1}^p(t)\ dt\right]_{i_1,j_1=1}^{n+p}, \tag{2.8}$$

$$S_n^p = \left[\int_0^1 \left(N_{i_1}^p(t)\right)'\ \left(N_{j_1}^p(t)\right)'\ dt\right]_{i_1,j_1=1}^{n+p}. \tag{2.9}$$

We know that M_n^p are symmetric positive definite matrices and S_n^p are symmetric positive semidefinite matrices (see, e.g., [7]). Furthermore, using the results of Subsection 2.1, these matrices can be expressed as

$$\begin{aligned}(M_n^p)_{i_1 j_1} &= \frac{1}{n}\ \phi_{2p+1}(p+1-(i_1-j_1)),\\ (S_n^p)_{i_1 j_1} &= -\,n\phi''_{2p+1}(p+1-(i_1-j_1)),\end{aligned}$$

up to a low-rank perturbation (see [8,9]), that is, they are low-rank perturbations of Toeplitz matrices. Thanks to the results in Subsection 2.3, the following theorems on the symbol of the sequences of mass and stiffness matrices in (2.8)–(2.9) hold.

Theorem 2.12. *$\{nM_n^p\}_n \sim_{\text{GLT}} \mathfrak{m}_p$ and $\{nM_n^p\}_n \sim_{\sigma,\lambda} (\mathfrak{m}_p, [-\pi,\pi])$, where the symbol $\mathfrak{m}_p$ is given by*

$$\mathfrak{m}_p(x,\theta) := \mathfrak{m}_p(\theta) = \phi_{2p+1}(p+1) + 2\sum_{k=1}^{p} \phi_{2p+1}(p+1-k)\cos(k\theta).$$

Theorem 2.13. *$\left\{\frac{1}{n}S_n^p\right\}_n \sim_{\text{GLT}} \mathfrak{s}_p$ and $\left\{\frac{1}{n}S_n^p\right\}_n \sim_{\sigma,\lambda} (\mathfrak{s}_p, [-\pi,\pi])$, where the symbol $\mathfrak{s}_p$ is given by*

$$\mathfrak{s}_p(x,\theta) := \mathfrak{s}_p(\theta) = -\phi''_{2p+1}(p+1) - 2\sum_{k=1}^{p} \phi''_{2p+1}(p+1-k)\cos(k\theta).$$

The symbols $\mathfrak{m}_p(\theta)$ and $\mathfrak{s}_p(\theta)$ satisfy the following properties for all $p \geq 1$ and $\theta \in [-\pi,\pi]$ (see [5,7]):

c1) $\mathfrak{s}_p(\theta) = \mathfrak{m}_{p-1}(\theta)(2-2\cos(\theta))$;

c2) Let $M_{\mathfrak{s}_p} = \max_{[0,\pi]} \mathfrak{s}_p(\theta)$. Then

$$\frac{\mathfrak{s}_p(\pi)}{M_{\mathfrak{s}_p}} \leq 2^{2-p},$$

which means that $\frac{\mathfrak{s}_p(\pi)}{M_{\mathfrak{s}_p}}$ decreases exponentially to zero as $p \to \infty$;

c3) $\left(\frac{4}{\pi^2}\right)^p \leq \mathfrak{m}_p(\theta) \leq \mathfrak{m}_p(0) = 1$.

Remark 2.14. As a result of the previous properties, the function $\mathfrak{s}_p(\theta)$ has a unique zero of order 2 at 0 (like the function $2-2\cos(\theta)$). On the other hand, from a numerical point of view, we can say that, for large p, the normalized symbol $\frac{\mathfrak{s}_p(\theta)}{M_{\mathfrak{s}_p}}$ has also an exponential numerical zero at $\theta = \pi$.

3. IgA discretization of curl-curl operator

In [2], the construction of a discrete de Rham sequence using B-splines is established, which provides the following commutative diagram:

$$\begin{array}{ccccccc}
H^1(\Omega) & \xrightarrow{\boldsymbol{\nabla}} & \boldsymbol{H}(\mathrm{curl},\Omega) & \xrightarrow{\nabla\times} & \boldsymbol{H}(\mathrm{div},\Omega) & \xrightarrow{\nabla\cdot} & L^2(\Omega) \\
\downarrow{\scriptstyle \boldsymbol{\Pi}_h^{\mathrm{grad}}} & & \downarrow{\scriptstyle \boldsymbol{\Pi}_h^{\mathrm{curl}}} & & \downarrow{\scriptstyle \boldsymbol{\Pi}_h^{\mathrm{div}}} & & \downarrow{\scriptstyle \boldsymbol{\Pi}_h^{L^2}} \\
V_h(\mathrm{grad},\Omega) & \xrightarrow{\boldsymbol{\nabla}} & \boldsymbol{V}_h(\mathrm{curl},\Omega) & \xrightarrow{\nabla\times} & \boldsymbol{V}_h(\mathrm{div},\Omega) & \xrightarrow{\nabla\cdot} & V_h(L^2,\Omega)
\end{array}$$

In the 2D case, the previous diagram is reduced to 2 diagrams. For this work, we are concerned with the following commuting diagram:

$$\begin{array}{ccccc}
H^1(\Omega) & \xrightarrow{\boldsymbol{\nabla}} & \boldsymbol{H}(\mathrm{curl},\Omega) & \xrightarrow{\nabla\times} & L^2(\Omega) \\
\downarrow{\scriptstyle \boldsymbol{\Pi}_h^{\mathrm{grad}}} & & \downarrow{\scriptstyle \boldsymbol{\Pi}_h^{\mathrm{curl}}} & & \downarrow{\scriptstyle \boldsymbol{\Pi}_h^{L^2}} \\
V_h(\mathrm{grad},\Omega) & \xrightarrow{\boldsymbol{\nabla}} & \boldsymbol{V}_h(\mathrm{curl},\Omega) & \xrightarrow{\nabla\times} & V_h(L^2,\Omega),
\end{array}$$

where

$$V_h(\mathrm{grad},\Omega) = S^{p,p}, \quad \boldsymbol{V}_h(\mathrm{curl},\Omega) = \begin{pmatrix} S^{p-1,p} \\ S^{p,p-1} \end{pmatrix}, \quad \text{and} \quad V_h(L^2,\Omega) = S^{p-1,p-1}.$$

More precisely,

$$\boldsymbol{V}_h(\mathrm{curl},\Omega) = S^{p-1,p} \times S^{p,p-1} = \mathrm{span}\{\boldsymbol{\psi}^1_{i_1,i_2}, \boldsymbol{\psi}^2_{j_1,j_2}\}_{i_1,i_2,j_1,j_2},$$

where $S^{p-1,p}$ and $S^{p,p-1}$ are defined as in (2.4), namely:

$$S^{p-1,p} := \mathrm{span}\left\{N^{p-1}_{i_1}(t_1)N^p_{i_2}(t_2)\right\}_{i_1,i_2}, \quad i_1 = 1,\dots,n_1+p-1, \quad i_2 = 1,\dots,n_2+p,$$

$$S^{p,p-1} := \mathrm{span}\left\{N^p_{j_1}(t_1)N^{p-1}_{j_2}(t_2)\right\}_{j_1,j_2}, \quad j_1 = 1,\dots,n_1+p, \quad j_2 = 1,\dots,n_2+p-1,$$

$$\boldsymbol{\psi}^1_{i_1,i_2} = \begin{bmatrix} N^{p-1}_{i_1}(t_1)N^p_{i_2}(t_2) \\ 0 \end{bmatrix}, \qquad \boldsymbol{\psi}^2_{j_1,j_2} = \begin{bmatrix} 0 \\ N^p_{j_1}(t_1)N^{p-1}_{j_2}(t_2) \end{bmatrix}.$$

Problem (1.1) at the discrete level then reads as:

$$\text{(3.1)} \quad \boldsymbol{u} \in \boldsymbol{V}_h(\mathrm{curl},\Omega): \quad (\nabla\times\boldsymbol{u}, \nabla\times\boldsymbol{v}) + \mu\,(\boldsymbol{u},\boldsymbol{v}) = (\boldsymbol{f},\boldsymbol{v}), \quad \forall \boldsymbol{v} \in \boldsymbol{V}_h(\mathrm{curl},\Omega),$$

Remark 3.1. Boundary contributions are considered to be included in the right-hand side term $\boldsymbol{f}$. Therefore, no essential boundary conditions are imposed in the construction of the Finite Elements space, and all the degrees of freedom are taken into account here. Moreover, weak boundary conditions such as those related to Nitsche's method, are not considered in the current paper and may be covered in a future work.

Using the expansion

$$\boldsymbol{u} = \begin{bmatrix} \sum_{i_1=1}^{n_1+p-1}\sum_{i_2=1}^{n_2+p} u^1_{i_1,i_2} N^{p-1}_{i_1}(t_1)N^p_{i_2}(t_2) \\ \\ \sum_{j_1=1}^{n_1+p}\sum_{j_2=1}^{n_2+p-1} u^2_{j_1,j_2} N^p_{j_1}(t_1)N^{p-1}_{j_2}(t_2) \end{bmatrix},$$

and choosing $\boldsymbol{v} = \boldsymbol{\psi}^1_{\tilde{i}_1,\tilde{i}_2}$, we obtain

$$\begin{aligned}
&(\nabla\times\boldsymbol{u}, \nabla\times\boldsymbol{\psi}^1_{\tilde{i}_1,\tilde{i}_2}) \\
&\quad = -\sum_{j_1=1}^{n_1+p}\sum_{j_2=1}^{n_2+p-1} u^2_{j_1,j_2} \int_\Omega \left(N^p_{j_1}(t_1)\right)' N^{p-1}_{j_2}(t_2) N^{p-1}_{\tilde{i}_1}(t_1) \left(N^p_{\tilde{i}_2}(t_2)\right)' dt_1 dt_2 \\
&\qquad + \sum_{i_1=1}^{n_1+p-1}\sum_{i_2=1}^{n_2+p} u^1_{i_1,i_2} \int_\Omega N^{p-1}_{i_1}(t_1) \left(N^p_{i_2}(t_2)\right)' N^{p-1}_{\tilde{i}_1}(t_1) \left(N^p_{\tilde{i}_2}(t_2)\right)' dt_1 dt_2, \\
&\quad = -\sum_{j_1=1}^{n_1+p}\sum_{j_2=1}^{n_2+p-1} u^2_{j_1,j_2} (A^p_{n_1} \otimes A^p_{n_2})_{\tilde{i}_1,\tilde{i}_2,j_1,j_2} \\
&\qquad + \sum_{i_1=1}^{n_1+p-1}\sum_{i_2=1}^{n_2+p} u^1_{i_1,i_2} (M^{p-1}_{n_1} \otimes S^p_{n_2})_{\tilde{i}_1,\tilde{i}_2,i_1,i_2},
\end{aligned} \tag{3.2}$$

where $M_{n_1}^{p-1}$ and $S_{n_2}^{p}$ are defined as in (2.8) and (2.9), i.e.,

$$(M_{n_1}^{p-1})_{\widetilde{i_1}i_1} = \int_0^1 N_{i_1}^{p-1}(t_1)N_{\widetilde{i_1}}^{p-1}(t_1)dt_1, \quad \widetilde{i_1}, i_1 = 1, \ldots, n_1+p-1,$$
$$(S_{n_2}^{p})_{\widetilde{i_2}i_2} = \int_0^1 \left(N_{i_2}^{p}(t_2)\right)' \left(N_{\widetilde{i_2}}^{p}(t_2)\right)' dt_2, \quad \widetilde{i_2}, i_2 = 1, \ldots, n_2+p,$$

while

$$(A_{n_1}^{p})_{\widetilde{i_1}j_1} = \int_0^1 N_{\widetilde{i_1}}^{p-1}(t_1)\left(N_{j_1}^{p}(t_1)\right)' dt_1, \begin{array}{l}\widetilde{i_1} = 1, \ldots, n_1+p-1,\\ j_1 = 1, \ldots, n_1+p,\end{array}$$
$$(A_{n_2}^{p})_{\widetilde{i_2}j_2} = \int_0^1 N_{j_2}^{p-1}(t_2)\left(N_{\widetilde{i_2}}^{p}(t_2)\right)' dt_2, \begin{array}{l}\widetilde{i_2} = 1, \ldots, n_2+p,\\ j_2 = 1, \ldots, n_2+p-1.\end{array}$$

Equation (3.2) can be expressed in compact form as follows:

$$M_{n_1}^{p-1} \otimes S_{n_2}^{p} u^1 - A_{n_1}^{p} \otimes A_{n_2}^{p} u^2. \tag{3.3}$$

On the other hand, if we choose $\boldsymbol{v} = \boldsymbol{\psi}^2_{\widetilde{j_1},\widetilde{j_2}}$, then we obtain

$$\begin{aligned}
&(\nabla \times \boldsymbol{u}, \nabla \times \boldsymbol{\psi}^2_{\widetilde{j_1},\widetilde{j_2}})\\
&\quad = \sum_{j_1=1}^{n_1+p}\sum_{j_2=1}^{n_2+p-1} u^2_{j_1,j_2} \int_\Omega \left(N_{j_1}^{p}(t_1)\right)' N_{j_2}^{p-1}(t_2) \left(N_{\widetilde{j_1}}^{p}(t_1)\right)' N_{\widetilde{j_2}}^{p-1}(t_2)dt_1dt_2\\
&\qquad - \sum_{i_1=1}^{n_1+p-1}\sum_{i_2=1}^{n_2+p} u^1_{i_1,i_2} \int_\Omega N_{i_1}^{p-1}(t_1)\left(N_{i_2}^{p}(t_2)\right)' \left(N_{\widetilde{j_1}}^{p}(t_1)\right)' N_{\widetilde{j_2}}^{p-1}(t_2)dt_1dt_2
\end{aligned} \tag{3.4}$$
$$\begin{aligned}
&\quad = \sum_{j_1=1}^{n_1+p}\sum_{j_2=1}^{n_2+p-1} u^2_{j_1,j_2}(S_{n_1}^{p} \otimes M_{n_2}^{p-1})_{\widetilde{j_1},\widetilde{j_2},j_1,j_2}\\
&\qquad - \sum_{i_1=1}^{n_1+p-1}\sum_{i_2=1}^{n_2+p} u^1_{i_1,i_2}(B_{n_1}^{p} \otimes B_{n_2}^{p})_{\widetilde{j_1},\widetilde{j_2},i_1,i_2},
\end{aligned}$$

where $M_{n_2}^{p-1}$ and $S_{n_1}^{p}$ are defined as in (2.8) and (2.9), i.e.,

$$(M_{n_2}^{p-1})_{\widetilde{j_2}j_2} = \int_0^1 N_{j_2}^{p-1}(t_2)N_{\widetilde{j_2}}^{p-1}(t_2)dt_2, \quad \widetilde{j_2}, j_2 = 1, \ldots, n_2+p-1,$$
$$(S_{n_1}^{p})_{\widetilde{j_1}j_1} = \int_0^1 \left(N_{j_1}^{p}(t_1)\right)' \left(N_{\widetilde{j_1}}^{p}(t_1)\right)' dt_1, \quad \widetilde{j_1}, j_1 = 1, \ldots, n_1+p,$$

while

$$B_{n_1}^{p} = (A_{n_1}^{p})^T,$$
$$B_{n_2}^{p} = (A_{n_2}^{p})^T.$$

Equation (3.4) can be rewritten in compact form as follows:

$$S_{n_1}^{p} \otimes M_{n_2}^{p-1} u^2 - (A_{n_1}^{p} \otimes A_{n_2}^{p})^T u^1. \tag{3.5}$$

Putting together equations (3.3) and (3.5), we obtain the following two-by-two matrix:

$$\mathcal{A}_{\boldsymbol{n}} = \begin{bmatrix} M_{n_1}^{p-1} \otimes S_{n_2}^{p} & -A_{n_1}^{p} \otimes A_{n_2}^{p} \\ -(A_{n_1}^{p} \otimes A_{n_2}^{p})^T & S_{n_1}^{p} \otimes M_{n_2}^{p-1} \end{bmatrix}. \tag{3.6}$$

Such a matrix is the result of the IgA discretization of the curl-curl operator $(\nabla \times \ \cdot, \nabla \times \cdot)$ appearing in problem (1.1). In order to complete the operator in the left-hand side of (1.1) by adding the zero-order term $\mu(\cdot,\cdot)$, we obtain the following two-by-two coefficient matrix for problem (3.1)

$$\mathcal{A}^{\mu}_{\boldsymbol{n}} = \mathcal{A}_{\boldsymbol{n}} + \mu \begin{bmatrix} M^{p-1}_{n_1} \otimes M^{p}_{n_2} & \mathbf{0} \\ \mathbf{0}^T & M^{p}_{n_1} \otimes M^{p-1}_{n_2} \end{bmatrix}, \tag{3.7}$$

where $\mathbf{0}$ is the null matrix of size $(n_1+p-1)(n_2+p) \times (n_1+p)(n_2+p-1)$. Note that according to our notation, $\mathcal{A}^{0}_{\boldsymbol{n}} \equiv \mathcal{A}_{\boldsymbol{n}}$.

Remark 3.2. In the general case in which $n_1 \neq n_2$ the blocks of $\mathcal{A}^{\mu}_{\boldsymbol{n}}$ have different sizes and the matrices on the antidiagonal are rectangular. On the contrary, if $n_1 = n_2$ all blocks are square matrices and have the same size. In spite of this, $A^{p}_{n_1}$ and $A^{p}_{n_2}$ are always rectangular matrices of size $(n_1+p-1) \times (n_1+p)$, $(n_2+p) \times (n_2+p-1)$, respectively.

4. Spectral analysis of $\{\mathcal{A}_{\boldsymbol{n}}\}_{\boldsymbol{n}}$, stabilizations, and computational proposals

The first aim of this section is to provide a spectral analysis of the matrix-sequences $\{\mathcal{A}_{\boldsymbol{n}}\}_{\boldsymbol{n}}$, $\{\mathcal{A}^{\mu}_{\boldsymbol{n}}\}_{\boldsymbol{n}}$ with $\mathcal{A}_{\boldsymbol{n}}$ and $\mathcal{A}^{\mu}_{\boldsymbol{n}}$ defined as (3.6) and (3.7), respectively. Because of the rectangular nature of the matrices on the antidiagonal of $\mathcal{A}_{\boldsymbol{n}}$, to compute the symbol of the matrix-sequence $\{\mathcal{A}_{\boldsymbol{n}}\}_{\boldsymbol{n}}$, we need to look at a bigger matrix $\widetilde{\mathcal{A}}_{\boldsymbol{n}}$, whose blocks are square matrices with same size, and then to use a sort of interlacing theorem for symbols (Theorem 4.3), for recovering the spectral information on the original matrix-sequence. Let us build the matrix $\widetilde{\mathcal{A}}_{\boldsymbol{n}}$ as follows:

$$\widetilde{\mathcal{A}}_{\boldsymbol{n}} = \begin{bmatrix} \widetilde{\mathcal{A}}^{(1,1)}_{\boldsymbol{n}} & \widetilde{\mathcal{A}}^{(1,2)}_{\boldsymbol{n}} \\ \widetilde{\mathcal{A}}^{(2,1)}_{\boldsymbol{n}} & \widetilde{\mathcal{A}}^{(2,2)}_{\boldsymbol{n}} \end{bmatrix} = \begin{bmatrix} \widetilde{M}^{p-1}_{n_1} \otimes S^{p}_{n_2} & -\widetilde{A}^{p}_{n_1} \otimes \widetilde{A}^{p}_{n_2} \\ -(\widetilde{A}^{p}_{n_1} \otimes \widetilde{A}^{p}_{n_2})^T & S^{p}_{n_1} \otimes \widetilde{M}^{p-1}_{n_2} \end{bmatrix},$$

where

$$\begin{aligned}
(\widetilde{M}^{p-1}_{n_1})_{ij} &= \int_0^1 N^{p-1}_i(t_1) N^{p-1}_j(t_1) dt_1, \quad i,j = 1,\dots,n_1+p, \\
(\widetilde{M}^{p-1}_{n_2})_{hk} &= \int_0^1 N^{p-1}_k(t_2) N^{p-1}_h(t_2) dt_2, \quad h,k = 1,\dots,n_2+p, \\
(\widetilde{A}^{p}_{n_1})_{ij} &= \int_0^1 N^{p-1}_i(t_1) \left(N^{p}_j(t_1)\right)' dt_1, \quad i,j = 1,\dots,n_1+p, \\
(\widetilde{A}^{p}_{n_2})_{hk} &= \int_0^1 N^{p-1}_k(t_2) \left(N^{p}_h(t_2)\right)' dt_2, \quad h,k = 1,\dots,n_2+p.
\end{aligned}$$

Remark 4.1. The new matrices assume the construction of additional B-splines. In order to keep the same spline space, the new spline of degree $p-1$ is associated to the knots $[t_{p+n+1}, \cdots t_{2p+n+1}]$ and therefore it is identically equal to zero. Notice, that any additional B-spline is admissible since our study only takes into account the internal knots.

More precisely, our strategy is the following:

- compute the symbol of $\{\widetilde{\mathcal{A}}_{\boldsymbol{n}}\}_{\boldsymbol{n}}$ by computing the symbol of each block $\{\widetilde{\mathcal{A}}^{(i,j)}_{\boldsymbol{n}}\}_{\boldsymbol{n}}$, $i,j = 1,2$;

- use the knowledge of the symbol of $\{\widetilde{\mathcal{A}}_{\boldsymbol{n}}\}_{\boldsymbol{n}}$ to retrieve the symbol of the original matrix-sequence $\{\mathcal{A}_{\boldsymbol{n}}\}_{\boldsymbol{n}}$ and then of $\{\mathcal{A}^{\mu}_{\boldsymbol{n}}\}_{\boldsymbol{n}}$.

Both steps require Theorem 4.3, which in turn needs Lemma 4.2. These two tools are of general interest and therefore a specific subsection is dedicated to them.

4.1. **Distribution tools: An extradimensional approach.** In this subsection we first extend the set of possible test functions (following an idea in [23]) and then connect the distribution of a sequence of matrices and of specific subsequences, constructed using principal submatrices with given constraints on the dimension (see Theorem 4.3). The idea is to overcome the difficulty encountered in studying the matrices $\mathcal{A}_{\boldsymbol{n}}$ and $\mathcal{A}^{\mu}_{\boldsymbol{n}}$, due to the presence of rectangular blocks: the strategy consists in "enlarging" the considered matrices for having square blocks, in deducing by GLT tools the distribution of the enlarged matrix-sequence, and finally in obtaining the distribution of $\{\mathcal{A}_{\boldsymbol{n}}\}_{\boldsymbol{n}}$, $\{\mathcal{A}^{\mu}_{\boldsymbol{n}}\}_{\boldsymbol{n}}$ via Theorem 4.3.

Lemma 4.2. *If* $\{A_{\boldsymbol{n}}\}_{\boldsymbol{n}} \sim_\lambda (f, G)$ *with* $A_{\boldsymbol{n}}$ *Hermitian matrix such that* $\dim(A_{\boldsymbol{n}}) = d_{\boldsymbol{n}}$, $d_{\boldsymbol{n}} \to \infty$ *as* $\boldsymbol{n} \to \infty$ *and* f *and* G *as in Definition* 2.6*, then for every* F *continuous and bounded on* $\mathbb{R}$*,*

$$\lim_{\boldsymbol{n}\to\infty} \frac{1}{d_{\boldsymbol{n}}} \sum_{j=1}^{d_{\boldsymbol{n}}} F(\lambda_j(A_{\boldsymbol{n}})) = \frac{1}{m_l(G)} \int_G \frac{\sum_{i=1}^{s} F(\lambda_i(f(\boldsymbol{t})))}{s} d\boldsymbol{t} =: \phi(F).$$

Proof. We want to prove that

$$\left| \frac{1}{d_{\boldsymbol{n}}} \sum_{j=1}^{d_{\boldsymbol{n}}} F(\lambda_j(A_{\boldsymbol{n}})) - \phi(F) \right| \tag{4.1}$$

tends to 0 as $\boldsymbol{n} \to \infty$. Let us start observing that for every F continuous and bounded on $\mathbb{R}$ there exists a sequence $\{F_m\}_m$ such that

(1) $F_m \in \mathcal{C}_0(\mathbb{R})$,
(2) $F_m \to F$ as $m \to \infty$ (pointwise convergence),
(3) $\|F_m\|_\infty \le \|F\|_\infty$.

For example, we can choose $F_m = F\psi_m$ with

$$\psi_m(x) = \begin{cases} 1, & \text{if } x \in [-m, m], \\ 0, & \text{if } x \notin [-m-1, m+1], \\ \text{between } (0,1) \text{ and such that } \psi_m \text{ is continuous,} & \text{otherwise.} \end{cases}$$

Let us rewrite relation (4.1) as follows:

$$\begin{aligned} \left| \frac{1}{d_{\boldsymbol{n}}} \sum_{j=1}^{d_{\boldsymbol{n}}} F(\lambda_j(A_{\boldsymbol{n}})) - \phi(F) \right| &\le \left| \frac{1}{d_{\boldsymbol{n}}} \sum_{j=1}^{d_{\boldsymbol{n}}} F(\lambda_j(A_{\boldsymbol{n}})) - \frac{1}{d_{\boldsymbol{n}}} \sum_{j=1}^{d_{\boldsymbol{n}}} F_m(\lambda_j(A_{\boldsymbol{n}})) \right| \\ &\quad + \left| \frac{1}{d_{\boldsymbol{n}}} \sum_{j=1}^{d_{\boldsymbol{n}}} F_m(\lambda_j(A_{\boldsymbol{n}})) - \phi(F_m) \right| + |\phi(F_m) - \phi(F)| \end{aligned} \tag{4.2}$$

and let us focus our attention on the first term on the right-hand side of (4.2). Using (3) and the hypothesis $\{A_{\boldsymbol{n}}\}_{\boldsymbol{n}} \sim_\lambda (f, G)$ we obtain

$$\left|\frac{1}{d_{\boldsymbol{n}}}\sum_{j=1}^{d_{\boldsymbol{n}}} F(\lambda_j(A_{\boldsymbol{n}})) - \frac{1}{d_{\boldsymbol{n}}}\sum_{j=1}^{d_{\boldsymbol{n}}} F_m(\lambda_j(A_{\boldsymbol{n}}))\right| \le \|F - F_m\|_\infty \frac{\#\{j : \lambda_j(A_{\boldsymbol{n}}) \notin [-m, m]\}}{d_{\boldsymbol{n}}}$$
$$\le 2\|F\|_\infty r(m)$$

with $r(m) \to 0$ as $m \to \infty$ (we refer the reader to paper [22, Lemma 2.2 and Section 2.2] for a detailed explanation). Thanks to item (1) and using again the hypothesis, we deduce that the second term on the right-hand side of (4.2) tends to zero for every fixed m and for $\boldsymbol{n} \to \infty$. Moreover, because of (2) and (3) we can apply the dominated convergence theorem to conclude that the third term on the right-hand side of (4.2) tends to zero for $m \to \infty$, independently of $\boldsymbol{n}$. Therefore,

$$\limsup_{\boldsymbol{n}\to\infty} \left|\frac{1}{d_{\boldsymbol{n}}}\sum_{j=1}^{d_{\boldsymbol{n}}} F(\lambda_j(A_{\boldsymbol{n}})) - \phi(F)\right| \le 2\|F\|_\infty r(m) + |\phi(F_m) - \phi(F)|$$

and then passing to the limit as $m \to \infty$ the proof is complete. □

We note that Lemma 4.2 can be seen as an extension to a generic sequence of Hermitian matrices of the results for Toeplitz sequences contained in [23]: in that paper for $f \in L^q$ it is shown that the test functions F have to be continuous and with a growth bound indicated by the relation $|F(z)| \le c|z|^q$ for some constant c with $q \ge 1$. The argument shown in Lemma 4.2 shows that a generalization is possible also for $q \in [0, 1]$, where case $q = 0$ is exactly the one considered in the previous lemma, by identifying the set of measurable functions with L^0.

Now, we will use it to prove the following theorem.

Theorem 4.3. *Let $\{\widetilde{A}_{\boldsymbol{n}}\}_{\boldsymbol{n}}$ be a sequence of Hermitian matrices with $\dim(\widetilde{A}_{\boldsymbol{n}}) = d_{\boldsymbol{n}}$, $d_{\boldsymbol{n}} \to \infty$ as $\boldsymbol{n} \to \infty$ and let f and G as in Definition 2.6. Define $A_{\boldsymbol{n}} = \mathcal{P}_{\boldsymbol{n}}^H \widetilde{A}_{\boldsymbol{n}} \mathcal{P}_{\boldsymbol{n}}$, with $\mathcal{P}_{\boldsymbol{n}} \in \mathbb{C}^{d_{\boldsymbol{n}} \times \delta_{\boldsymbol{n}}}$, $\delta_{\boldsymbol{n}} < d_{\boldsymbol{n}}$, and $\mathcal{P}_{\boldsymbol{n}}^H \mathcal{P}_{\boldsymbol{n}} = I_{\delta_{\boldsymbol{n}}}$. If*

$$\lim_{\boldsymbol{n}\to\infty} \frac{\delta_{\boldsymbol{n}}}{d_{\boldsymbol{n}}} = 1, \tag{4.3}$$

then

$$\{\widetilde{A}_{\boldsymbol{n}}\}_{\boldsymbol{n}} \sim_\lambda (f, G) \iff \{A_{\boldsymbol{n}}\}_{\boldsymbol{n}} \sim_\lambda (f, G).$$

Proof. Throughout the proof of this theorem, we assume the eigenvalues of $\widetilde{A}_{\boldsymbol{n}}$ and $A_{\boldsymbol{n}}$ to be ordered as follows:

$$\lambda_1(\widetilde{A}_{\boldsymbol{n}}) \ge \cdots \ge \lambda_{d_{\boldsymbol{n}}}(\widetilde{A}_{\boldsymbol{n}}), \qquad \lambda_1(A_{\boldsymbol{n}}) \ge \cdots \ge \lambda_{\delta_{\boldsymbol{n}}}(A_{\boldsymbol{n}}).$$

Let us observe that the thesis can be rewritten as follows: for every $F \in \mathcal{C}_0(\mathbb{R})$,

$$\left|\frac{1}{d_{\boldsymbol{n}}}\sum_{j=1}^{d_{\boldsymbol{n}}} F(\lambda_j(\widetilde{A}_{\boldsymbol{n}})) - \frac{1}{\delta_{\boldsymbol{n}}}\sum_{j=1}^{\delta_{\boldsymbol{n}}} F(\lambda_j(A_{\boldsymbol{n}}))\right| \tag{4.4}$$

tends to 0 as $\boldsymbol{n} \to 0$. It easy to convince the reader that $\forall F \in \mathcal{C}_0(\mathbb{R})$ and $\forall \epsilon > 0$ there exists $F_\epsilon \in \mathcal{C}_0^1(\mathbb{R})$ ($\mathcal{C}_0^1(\mathbb{R})$ is the space of functions in $C^1(\mathbb{R})$ with compact

support) such that $\|F - F_\epsilon\|_\infty < \epsilon$. This implies that

$$\begin{aligned}
&\left| \frac{1}{d_{\boldsymbol{n}}} \sum_{j=1}^{d_{\boldsymbol{n}}} F(\lambda_j(\widetilde{A}_{\boldsymbol{n}})) - \frac{1}{\delta_{\boldsymbol{n}}} \sum_{j=1}^{\delta_{\boldsymbol{n}}} F(\lambda_j(A_{\boldsymbol{n}})) \right| \\
&\quad \le \left| \frac{1}{d_{\boldsymbol{n}}} \sum_{j=1}^{d_{\boldsymbol{n}}} F(\lambda_j(\widetilde{A}_{\boldsymbol{n}})) - \frac{1}{d_{\boldsymbol{n}}} \sum_{j=1}^{d_{\boldsymbol{n}}} F_\epsilon(\lambda_j(\widetilde{A}_{\boldsymbol{n}})) \right| \\
&\qquad + \left| \frac{1}{d_{\boldsymbol{n}}} \sum_{j=1}^{d_{\boldsymbol{n}}} F_\epsilon(\lambda_j(\widetilde{A}_{\boldsymbol{n}})) - \frac{1}{\delta_{\boldsymbol{n}}} \sum_{j=1}^{\delta_{\boldsymbol{n}}} F_\epsilon(\lambda_j(A_{\boldsymbol{n}})) \right| \\
&\qquad + \left| \frac{1}{\delta_{\boldsymbol{n}}} \sum_{j=1}^{\delta_{\boldsymbol{n}}} F_\epsilon(\lambda_j(A_{\boldsymbol{n}})) - \frac{1}{\delta_{\boldsymbol{n}}} \sum_{j=1}^{\delta_{\boldsymbol{n}}} F(\lambda_j(A_{\boldsymbol{n}})) \right| \\
&\quad \le 2\epsilon + \left| \frac{1}{d_{\boldsymbol{n}}} \sum_{j=1}^{d_{\boldsymbol{n}}} F_\epsilon(\lambda_j(\widetilde{A}_{\boldsymbol{n}})) - \frac{1}{\delta_{\boldsymbol{n}}} \sum_{j=1}^{\delta_{\boldsymbol{n}}} F_\epsilon(\lambda_j(A_{\boldsymbol{n}})) \right|.
\end{aligned}$$

Moreover, $F_\epsilon \in \mathcal{C}_0^1(\mathbb{R})$ can be expressed as the difference between two nonnegative, nondecreasing, bounded functions:

$$F_\epsilon = F_\epsilon^+ - F_\epsilon^-,$$

hence,

$$\begin{aligned}
&\left| \frac{1}{d_{\boldsymbol{n}}} \sum_{j=1}^{d_{\boldsymbol{n}}} F_\epsilon(\lambda_j(\widetilde{A}_{\boldsymbol{n}})) - \frac{1}{\delta_{\boldsymbol{n}}} \sum_{j=1}^{\delta_{\boldsymbol{n}}} F_\epsilon(\lambda_j(A_{\boldsymbol{n}})) \right| \\
&\quad \le \left| \frac{1}{d_{\boldsymbol{n}}} \sum_{j=1}^{d_{\boldsymbol{n}}} F_\epsilon^+(\lambda_j(\widetilde{A}_{\boldsymbol{n}})) - \frac{1}{\delta_{\boldsymbol{n}}} \sum_{j=1}^{\delta_{\boldsymbol{n}}} F_\epsilon^+(\lambda_j(A_{\boldsymbol{n}})) \right| \\
&\qquad + \left| \frac{1}{d_{\boldsymbol{n}}} \sum_{j=1}^{d_{\boldsymbol{n}}} F_\epsilon^-(\lambda_j(\widetilde{A}_{\boldsymbol{n}})) - \frac{1}{\delta_{\boldsymbol{n}}} \sum_{j=1}^{\delta_{\boldsymbol{n}}} F_\epsilon^-(\lambda_j(A_{\boldsymbol{n}})) \right|,
\end{aligned}$$

which means that it is sufficient to prove the thesis when F is a nonnegative, nondecreasing, bounded function. To prove the necessary condition, we furnish a bound from above for (4.4) as follows:

$$\begin{aligned}
&\left| \frac{1}{d_{\boldsymbol{n}}} \sum_{j=1}^{d_{\boldsymbol{n}}} F(\lambda_j(\widetilde{A}_{\boldsymbol{n}})) - \frac{1}{\delta_{\boldsymbol{n}}} \sum_{j=1}^{\delta_{\boldsymbol{n}}} F(\lambda_j(A_{\boldsymbol{n}})) \right| \\
&\quad \le \left| \frac{1}{d_{\boldsymbol{n}}} \sum_{j=1}^{d_{\boldsymbol{n}}} F(\lambda_j(\widetilde{A}_{\boldsymbol{n}})) - \frac{1}{\delta_{\boldsymbol{n}}} \sum_{j=1}^{\delta_{\boldsymbol{n}}} F(\lambda_j(\widetilde{A}_{\boldsymbol{n}})) \right| \\
&\qquad + \left| \frac{1}{\delta_{\boldsymbol{n}}} \sum_{j=1}^{\delta_{\boldsymbol{n}}} F(\lambda_j(\widetilde{A}_{\boldsymbol{n}})) - \frac{1}{\delta_{\boldsymbol{n}}} \sum_{j=1}^{\delta_{\boldsymbol{n}}} F(\lambda_j(A_{\boldsymbol{n}})) \right|.
\end{aligned} \tag{4.5}$$

In order to give an upper bound for the first term in the right-hand side of (4.5) with a quantity which tends to 0 as $\boldsymbol{n} \to \infty$, we first observe that, using the hypothesis

$\{\widetilde{A}_{\boldsymbol{n}}\}_{\boldsymbol{n}} \sim_\lambda (f, G)$ and applying Lemma 4.2, we find

$$\lim_{\boldsymbol{n}\to\infty} \frac{1}{d_{\boldsymbol{n}}} \sum_{j=1}^{d_{\boldsymbol{n}}} F(\lambda_j(\widetilde{A}_{\boldsymbol{n}})) = \phi(F). \tag{4.6}$$

Moreover, from hypothesis (4.3), we deduce $\delta_{\boldsymbol{n}} = d_{\boldsymbol{n}} + o(d_{\boldsymbol{n}})$ and then

$$\lim_{\boldsymbol{n}\to\infty} \frac{1}{\delta_{\boldsymbol{n}}} \sum_{j=1}^{\delta_{\boldsymbol{n}}} F(\lambda_j(\widetilde{A}_{\boldsymbol{n}})) = \phi(F). \tag{4.7}$$

Putting together (4.6) and (4.7), we can conclude that the first term in the right-hand side of (4.5) can be bounded from above by a quantity which tends to 0 as $\boldsymbol{n} \to \infty$. Concerning the second term in the right-hand side of (4.5), we start by defining

$$\begin{aligned} a_{\boldsymbol{n}} &= \sum_{j=1}^{\delta_{\boldsymbol{n}}} F(\lambda_j(\widetilde{A}_{\boldsymbol{n}})), \\ b_{\boldsymbol{n}} &= \sum_{j=1}^{\delta_{\boldsymbol{n}}} F(\lambda_j(A_{\boldsymbol{n}})), \\ c_{\boldsymbol{n}} &= \sum_{j=1+d_{\boldsymbol{n}}-\delta_{\boldsymbol{n}}}^{d_{\boldsymbol{n}}} F(\lambda_j(\widetilde{A}_{\boldsymbol{n}})). \end{aligned}$$

Thanks to the Cauchy interlacing theorem (see, e.g., [1]), we know that

$$\lambda_j(\widetilde{A}_{\boldsymbol{n}}) \geq \lambda_j(A_{\boldsymbol{n}}) \geq \lambda_{j+d_{\boldsymbol{n}}-\delta_{\boldsymbol{n}}}(\widetilde{A}_{\boldsymbol{n}}), \qquad j = 1, \ldots, \delta_{\boldsymbol{n}}.$$

From the monotonicity of F and from the Cauchy interlacing theorem, we find

$$a_{\boldsymbol{n}} \geq b_{\boldsymbol{n}} \geq c_{\boldsymbol{n}}.$$

Both $a_{\boldsymbol{n}}/\delta_{\boldsymbol{n}}$ and $c_{\boldsymbol{n}}/\delta_{\boldsymbol{n}}$ tend to the limit given in (4.7). This implies that $b_{\boldsymbol{n}}/\delta_{\boldsymbol{n}}$ converges to the same limit and the necessary condition is proved.

To prove the sufficient condition, we start from the quantity (4.4), by taking into account the following inequality:

$$\begin{aligned} &\left| \frac{1}{d_{\boldsymbol{n}}} \sum_{j=1}^{d_{\boldsymbol{n}}} F(\lambda_j(\widetilde{A}_{\boldsymbol{n}})) - \frac{1}{\delta_{\boldsymbol{n}}} \sum_{j=1}^{\delta_{\boldsymbol{n}}} F(\lambda_j(A_{\boldsymbol{n}})) \right| \\ &\qquad \leq \left| \frac{1}{d_{\boldsymbol{n}}} \sum_{j=1}^{d_{\boldsymbol{n}}} F(\lambda_j(\widetilde{A}_{\boldsymbol{n}})) - \frac{1}{d_{\boldsymbol{n}}} \sum_{j=1}^{\delta_{\boldsymbol{n}}} F(\lambda_j(A_{\boldsymbol{n}})) \right| \\ &\qquad\quad + \left| \frac{1}{d_{\boldsymbol{n}}} \sum_{j=1}^{\delta_{\boldsymbol{n}}} F(\lambda_j(A_{\boldsymbol{n}})) - \frac{1}{\delta_{\boldsymbol{n}}} \sum_{j=1}^{\delta_{\boldsymbol{n}}} F(\lambda_j(A_{\boldsymbol{n}})) \right|. \end{aligned} \tag{4.8}$$

In order to bound from above the first term in the right-hand side of (4.8), we use the Cauchy interlacing theorem and we obtain

$$\frac{1}{d_{\boldsymbol{n}}} \sum_{j=1}^{d_{\boldsymbol{n}}} F(\lambda_j(\widetilde{A}_{\boldsymbol{n}})) \geq \frac{1}{d_{\boldsymbol{n}}} \sum_{j=1}^{\delta_{\boldsymbol{n}}} F(\lambda_j(A_{\boldsymbol{n}})) \geq \frac{1}{d_{\boldsymbol{n}}} \sum_{j=1}^{\delta_{\boldsymbol{n}}} F(\lambda_{j+d_{\boldsymbol{n}}-\delta_{\boldsymbol{n}}}(\widetilde{A}_{\boldsymbol{n}})).$$

Consequently,

$$\begin{aligned}
&\left|\frac{1}{d_{\boldsymbol{n}}}\sum_{j=1}^{d_{\boldsymbol{n}}}F(\lambda_j(\widetilde{A}_{\boldsymbol{n}}))-\frac{1}{d_{\boldsymbol{n}}}\sum_{j=1}^{\delta_{\boldsymbol{n}}}F(\lambda_j(A_{\boldsymbol{n}}))\right|\\
&\quad=\frac{1}{d_{\boldsymbol{n}}}\sum_{j=1}^{d_{\boldsymbol{n}}}F(\lambda_j(\widetilde{A}_{\boldsymbol{n}}))-\frac{1}{d_{\boldsymbol{n}}}\sum_{j=1}^{\delta_{\boldsymbol{n}}}F(\lambda_j(A_{\boldsymbol{n}}))\\
&\quad\le\frac{1}{d_{\boldsymbol{n}}}\sum_{j=1}^{d_{\boldsymbol{n}}}F(\lambda_j(\widetilde{A}_{\boldsymbol{n}}))-\frac{1}{d_{\boldsymbol{n}}}\sum_{j=1+d_{\boldsymbol{n}}-\delta_{\boldsymbol{n}}}^{d_{\boldsymbol{n}}}F(\lambda_j(\widetilde{A}_{\boldsymbol{n}}))\\
&\quad=\frac{1}{d_{\boldsymbol{n}}}\sum_{j=1}^{d_{\boldsymbol{n}}-\delta_{\boldsymbol{n}}}F(\lambda_j(\widetilde{A}_{\boldsymbol{n}}))\le\frac{1}{d_{\boldsymbol{n}}}\sum_{j=1}^{d_{\boldsymbol{n}}-\delta_{\boldsymbol{n}}}\|F\|_\infty\\
&\quad=\frac{d_{\boldsymbol{n}}-\delta_{\boldsymbol{n}}}{d_{\boldsymbol{n}}}\|F\|_\infty.
\end{aligned}$$

Thanks to hypothesis (4.3), we can conclude that the first term in the right-hand side of (4.8) can be bounded from above by a quantity which tends to 0 as $\boldsymbol{n}\to\infty$. As a consequence of hypothesis $\{A_{\boldsymbol{n}}\}_{\boldsymbol{n}}\sim_\lambda(f,G)$, of the fact that $d_{\boldsymbol{n}}-\delta_{\boldsymbol{n}}=o(d_{\boldsymbol{n}})$, and of Lemma 4.2, the same is true also for the second term in the right-hand side of (4.8) and the proof of the theorem is complete. □

We end this subsection by observing that Theorem 4.3 can be extended to sequences of non-Hermitian matrices and related sequences of principal submatrices, when replacing the eigenvalue distribution with the singular value one. See the following corollary and the given proof sketch.

Corollary 4.4. *Let $\{\widetilde{A}_{\boldsymbol{n}}\}_{\boldsymbol{n}}$ be a sequence of matrices with $\dim(\widetilde{A}_{\boldsymbol{n}})=d_{\boldsymbol{n}}$, $d_{\boldsymbol{n}}\to\infty$ as $\boldsymbol{n}\to\infty$ and let f and G as in Definition 2.6. Define $A_{\boldsymbol{n}}=\mathcal{P}_{\boldsymbol{n}}^H\widetilde{A}_{\boldsymbol{n}}\mathcal{P}_{\boldsymbol{n}}$, with $\mathcal{P}_{\boldsymbol{n}}\in\mathbb{C}^{d_{\boldsymbol{n}}\times\delta_{\boldsymbol{n}}}$, $\delta_{\boldsymbol{n}}<d_{\boldsymbol{n}}$, and $\mathcal{P}_{\boldsymbol{n}}^H\mathcal{P}_{\boldsymbol{n}}=I_{\delta_{\boldsymbol{n}}}$. If relation (4.3) holds, then*

$$\{\widetilde{A}_{\boldsymbol{n}}\}_{\boldsymbol{n}}\sim_\sigma(f,G)\iff\{A_{\boldsymbol{n}}\}_{\boldsymbol{n}}\sim_\sigma(f,G).$$

Proof. For any matrix $\widetilde{A}_{\boldsymbol{n}}$ with $\dim(\widetilde{A}_{\boldsymbol{n}})=d_{\boldsymbol{n}}$ and any principal submatrix $A_{\boldsymbol{n}}=\mathcal{P}_{\boldsymbol{n}}^H\widetilde{A}_{\boldsymbol{n}}\mathcal{P}_{\boldsymbol{n}}$ of $\widetilde{A}_{\boldsymbol{n}}$ with $\dim(A_{\boldsymbol{n}})=\delta_{\boldsymbol{n}}<d_{\boldsymbol{n}}$ satisfying (4.3) let us consider the following block matrices of double size

$$\widetilde{B}_{\boldsymbol{n}}=\begin{bmatrix}\mathbf{0}&\widetilde{A}_{\boldsymbol{n}}^H\\ \widetilde{A}_{\boldsymbol{n}}&\mathbf{0}\end{bmatrix}\in\mathbb{C}^{2d_{\boldsymbol{n}}\times2d_{\boldsymbol{n}}},\quad B_{\boldsymbol{n}}=\begin{bmatrix}\mathbf{0}&A_{\boldsymbol{n}}^H\\ A_{\boldsymbol{n}}&\mathbf{0}\end{bmatrix}\in\mathbb{C}^{2\delta_{\boldsymbol{n}}\times2\delta_{\boldsymbol{n}}}.$$

By construction, both $\widetilde{B}_{\boldsymbol{n}}$ and $B_{\boldsymbol{n}}$ are Hermitian matrices. Moreover, $B_{\boldsymbol{n}}$ is a principal submatrix of $\widetilde{B}_{\boldsymbol{n}}$ such that relation (4.3) holds. Indeed, if we define

$$\mathcal{P}_{\boldsymbol{n}}^{[2]}=\begin{bmatrix}\mathcal{P}_{\boldsymbol{n}}&\mathbf{0}\\ \mathbf{0}&\mathcal{P}_{\boldsymbol{n}}\end{bmatrix}\in\mathbb{C}^{2d_{\boldsymbol{n}}\times2\delta_{\boldsymbol{n}}},$$

then $B_{\boldsymbol{n}}=(\mathcal{P}_{\boldsymbol{n}}^{[2]})^H\widetilde{B}_{\boldsymbol{n}}\mathcal{P}_{\boldsymbol{n}}^{[2]}$ and $(\mathcal{P}_{\boldsymbol{n}}^{[2]})^H\mathcal{P}_{\boldsymbol{n}}^{[2]}=I_{2\delta_{\boldsymbol{n}}}$. Therefore, thanks to Theorem 4.3 we have that

$$\{\widetilde{B}_{\boldsymbol{n}}\}_{\boldsymbol{n}}\sim_\lambda(f,G)\iff\{B_{\boldsymbol{n}}\}_{\boldsymbol{n}}\sim_\lambda(f,G).$$

On the other hand, it is well known that the eigenvalues of $\widetilde{B}_{\boldsymbol{n}}$ are given by

$$\begin{aligned}\lambda_j(\widetilde{B}_{\boldsymbol{n}}) &= \sigma_j(\widetilde{A}_{\boldsymbol{n}}),\\ \lambda_{d_{\boldsymbol{n}}+j}(\widetilde{B}_{\boldsymbol{n}}) &= -\sigma_{d_{\boldsymbol{n}}-j+1}(\widetilde{A}_{\boldsymbol{n}}),\end{aligned} \qquad j=1,\dots,d_{\boldsymbol{n}},$$

with both $\lambda_j(\widetilde{B}_{\boldsymbol{n}})$ and $\sigma_j(\widetilde{A}_{\boldsymbol{n}})$ arranged in nonincreasing order. Similarly, the eigenvalues of $B_{\boldsymbol{n}}$ are given by

$$\begin{aligned}\lambda_j(B_{\boldsymbol{n}}) &= \sigma_j(A_{\boldsymbol{n}}),\\ \lambda_{\delta_{\boldsymbol{n}}+j}(B_{\boldsymbol{n}}) &= -\sigma_{\delta_{\boldsymbol{n}}-j+1}(A_{\boldsymbol{n}}),\end{aligned} \qquad j=1,\dots,\delta_{\boldsymbol{n}},$$

with both $\lambda_j(B_{\boldsymbol{n}})$ and $\sigma_j(A_{\boldsymbol{n}})$ arranged in nonincreasing order. With these results in mind, it is straightforward to see that

$$\begin{aligned}\{\widetilde{B}_{\boldsymbol{n}}\}_{\boldsymbol{n}} \sim_\lambda (f,G) &\iff \{\widetilde{A}_{\boldsymbol{n}}\}_{\boldsymbol{n}} \sim_\sigma (f,G),\\ \{B_{\boldsymbol{n}}\}_{\boldsymbol{n}} \sim_\lambda (f,G) &\iff \{A_{\boldsymbol{n}}\}_{\boldsymbol{n}} \sim_\sigma (f,G),\end{aligned}$$

and the thesis is proved. □

4.2. **Spectral analysis of the matrices $\mathcal{A}_{\boldsymbol{n}}$ and $\mathcal{A}^{\mu}_{\boldsymbol{n}}$ by the extradimensional approach.** Here we come back to the study of the spectral distribution of $\{\widetilde{\mathcal{A}}_{\boldsymbol{n}}\}_{\boldsymbol{n}}$ and then of $\{\mathcal{A}_{\boldsymbol{n}}\}_{\boldsymbol{n}}$, by using the extradimensional approach (we borrowed the expression "extradimensional" from a conversation with Eugene Tyrtyshnikov more than 15 years ago). Indeed, thanks to Theorems 2.12, 2.13, and to property **c1)**, the following results hold:

$$\begin{aligned}&\{n_1 M_{n_1}^{p-1}\}_{n_1} \sim_\lambda (\mathfrak{m}_{p-1}(\theta_1),[-\pi,\pi]),\\ &\{n_2 M_{n_2}^{p-1}\}_{n_2} \sim_\lambda (\mathfrak{m}_{p-1}(\theta_2),[-\pi,\pi]),\end{aligned}$$

$$\left\{\frac{1}{n_1}S^p_{n_1}\right\}_{n_1} \sim_\lambda (\mathfrak{s}_p(\theta_1)=\mathfrak{m}_{p-1}(\theta_1)(2-2\cos(\theta_1)),[-\pi,\pi]), \tag{4.9}$$

$$\left\{\frac{1}{n_2}S^p_{n_2}\right\}_{n_2} \sim_\lambda (\mathfrak{s}_p(\theta_2)=\mathfrak{m}_{p-1}(\theta_2)(2-2\cos(\theta_2)),[-\pi,\pi]). \tag{4.10}$$

Note that

$$\begin{aligned}M_{n_1}^{p-1} &= H_1 \widetilde{M}_{n_1}^{p-1} H_1^T,\\ M_{n_2}^{p-1} &= H_2^T \widetilde{M}_{n_2}^{p-1} H_2,\end{aligned} \tag{4.11}$$

where

$$H_1 = \begin{bmatrix} I_1 & \mathbf{0}_1 \end{bmatrix} \tag{4.12}$$

with $\mathbf{0}_1=[0,\dots,0]^T\in\mathbb{R}^{n_1+p-1}$ and $I_1\in\mathbb{R}^{(n_1+p-1)\times(n_1+p-1)}$, while

$$H_2 = \begin{bmatrix} I_2 \\ \mathbf{0}_2 \end{bmatrix} \tag{4.13}$$

with $\mathbf{0}_2=[0,\dots,0]\in\mathbb{R}^{n_2+p-1}$ and $I_2\in\mathbb{R}^{(n_2+p-1)\times(n_2+p-1)}$. Because of relations (4.11), we can apply Theorem 4.3 to $\{n_1\widetilde{M}_{n_1}^{p-1}\}_{n_1}$ and $\{n_2\widetilde{M}_{n_2}^{p-1}\}_{n_2}$. Thus, by exploiting relations (4.9)–(4.10) and assuming $\boldsymbol{n}=(n_1,n_2)=(\nu_1,\nu_2)n$, $n\in\mathbb{N}$,

$\nu_1, \nu_2 \in \mathbb{Q}$, we obtain

$$\left\{\widetilde{\mathcal{A}}_{\boldsymbol{n}}^{(1,1)}\right\}_{\boldsymbol{n}} = \left\{\widetilde{M}_{n_1}^{p-1} \otimes S_{n_2}^{p}\right\}_{\boldsymbol{n}} \sim_\lambda \left(\frac{\nu_2}{\nu_1}\mathfrak{m}_{p-1}(\theta_1)\mathfrak{m}_{p-1}(\theta_2)(2-2\cos(\theta_2)), [-\pi,\pi]^2\right),$$

$$\left\{\widetilde{\mathcal{A}}_{\boldsymbol{n}}^{(2,2)}\right\}_{\boldsymbol{n}} = \left\{S_{n_1}^{p} \otimes \widetilde{M}_{n_2}^{p-1}\right\}_{\boldsymbol{n}} \sim_\lambda \left(\frac{\nu_1}{\nu_2}\mathfrak{m}_{p-1}(\theta_1)\mathfrak{m}_{p-1}(\theta_2)(2-2\cos(\theta_1)), [-\pi,\pi]^2\right).$$

With the aim of computing the symbol of blocks $\left\{\widetilde{\mathcal{A}}_{\boldsymbol{n}}^{(1,2)}\right\}_{\boldsymbol{n}}$ and $\left\{\widetilde{\mathcal{A}}_{\boldsymbol{n}}^{(2,1)}\right\}_{\boldsymbol{n}}$ let us start computing the symbol of $\{\widetilde{A}_{n_1}^{p}\}_{n_1}$. Thanks to the relations (2.2)–(2.3) between B-splines and cardinal B-splines, we know that

$$N_i^{p-1}(t_1) = \phi_{p-1}(n_1 t_1 - i + p), \quad i = p, \dots, n_1,$$
$$\left(N_j^{p}(t_1)\right)' = n_1 \phi_p'(n_1 t_1 - j + p + 1), \quad j = p+1, \dots, n_1.$$

Then we can write the principal submatrix of $\widetilde{A}_{n_1}^{p}$ corresponding to indices $p+1, \dots, n_1$ as follows:

$$\begin{aligned}\left[\widetilde{A}_{n_1}^{p}\right]_{i,j=p+1}^{n_1} &= n_1 \int_0^1 \phi_{p-1}(n_1 t_1 - i + p)\phi_p'(n_1 t_1 - j + p + 1)dt_1,\\ &= n_1 \int_{\mathbb{R}} \phi_{p-1}(n_1 t_1 - i + p)\phi_p'(n_1 t_1 - j + p + 1)dt_1,\\ &= \int_{\mathbb{R}} \phi_{p-1}(t_1)\phi_p'(t_1 + i - j + 1)dt_1.\end{aligned}$$

The second equality is obtained exploiting the local support property **b1)** for cardinal B-splines, while the last step is the result of the following change of variable $t_1 \to n_1 t_1 - i + p$. The entries of $[\widetilde{A}_{n_1}^{p}]_{i,j=p+1}^{n_1}$ depend only on the difference $i-j$, i.e., it is a Toeplitz matrix, and precisely

$$\left[\widetilde{A}_{n_1}^{p}\right]_{i,j=p+1}^{n_1} = T_{n_1-p}(\widetilde{\mathfrak{a}}_p),$$

where

$$\widetilde{\mathfrak{a}}_p(\theta_1) = \sum_{k\in\mathbb{Z}} \left(\int_{\mathbb{R}} \phi_{p-1}(t)\phi_p'(t+k+1)dt\right) \mathrm{e}^{\mathbf{i}k\theta_1}.$$

Making use of property **b3)** with $t+k+1$ in place of t, we obtain $\phi_p'(t+k+1) = \phi_{p-1}(t+k+1) - \phi_{p-1}(t+k)$. Hence $\widetilde{\mathfrak{a}}_p(\theta_1)$ can be rewritten as

$$\begin{aligned}\widetilde{\mathfrak{a}}_p(\theta_1) &= \sum_{k\in\mathbb{Z}} \left(\int_{\mathbb{R}} \phi_{p-1}(t)\phi_{p-1}(t+k+1)dt\right) \mathrm{e}^{\mathbf{i}k\theta_1}\\ &\quad - \sum_{k\in\mathbb{Z}} \left(\int_{\mathbb{R}} \phi_{p-1}(t)\phi_{p-1}(t+k)dt\right) \mathrm{e}^{\mathbf{i}k\theta_1}\\ &= \sum_{k\in\mathbb{Z}} \left(\int_{\mathbb{R}} \phi_{p-1}(t)\phi_{p-1}(t+k)dt\right) \mathrm{e}^{\mathbf{i}(k-1)\theta_1}\\ &\quad - \sum_{k\in\mathbb{Z}} \left(\int_{\mathbb{R}} \phi_{p-1}(t)\phi_{p-1}(t+k)dt\right) \mathrm{e}^{\mathbf{i}k\theta_1}\\ &= (\mathrm{e}^{-\mathbf{i}\theta_1} - 1) \sum_{k\in\mathbb{Z}} \left(\int_{\mathbb{R}} \phi_{p-1}(t)\phi_{p-1}(t+k)dt\right) \mathrm{e}^{\mathbf{i}k\theta_1}.\end{aligned}$$

By computing the inner product in the last equality and taking into account property **b6)**, with $r_1 = r_2 = 0$, $q_1 = q_2 = p-1$, and $\tau = k$, we deduce

$$\int_{\mathbb{R}} \phi_{p-1}(t)\phi_{p-1}(t+k)dt = \phi_{2p-1}(p-k),$$

which, by virtue of Theorem 2.12, implies the following identity:

$$\widetilde{\mathfrak{a}}_p(\theta_1) = \mathfrak{m}_{p-1}(\theta_1)(\mathrm{e}^{-\mathbf{i}\theta_1} - 1).$$

Note that $T_{n_1-p}(\widetilde{\mathfrak{a}}_p)$ is a principal submatrix of both $\widetilde{A}^p_{n_1}$ and $T_{n_1+p}(\widetilde{\mathfrak{a}}_p)$ and so

$$\widetilde{A}^p_{n_1} = T_{n_1+p}(\widetilde{\mathfrak{a}}_p) + R_{n_1}, \quad \operatorname{rank}(R_{n_1}) = o(n_1+p).$$

From Theorem 2.11, the sequence $\{R_{n_1}\}_{n_1}$ is a zero-distributed matrix-sequence, i.e, $\{R_{n_1}\}_{n_1} \sim_\sigma 0$ and therefore, by **GLT5**, $\{R_{n_1}\}_{n_1}$ is a GLT sequence with symbol identically zero. Using **GLT3**, also $\{T_{n_1+p}(\widetilde{\mathfrak{a}}_p)\}_{n_1}$ is a GLT sequence with symbol $\widetilde{\mathfrak{a}}_p$ and then, by **GLT2**, the sequence $\{T_{n_1+p}(\widetilde{\mathfrak{a}}_p) + R_{n_1}\}_{n_1}$ is still a GLT sequence with the same symbol. Consequently, by **GLT1**, we find

$$\{\widetilde{A}^p_{n_1}\}_{n_1} \sim_\sigma (\widetilde{\mathfrak{a}}_p(\theta_1), [-\pi,\pi]).$$

Similarly, we can prove that

$$\{\widetilde{A}^p_{n_2}\}_{n_2} \sim_\sigma (\widetilde{\mathfrak{a}}_p(-\theta_2), [-\pi,\pi]).$$

Therefore,

$$\left\{\widetilde{\mathcal{A}}^{(1,2)}_{\boldsymbol{n}}\right\}_{\boldsymbol{n}} = \left\{-\widetilde{A}^p_{n_1} \otimes \widetilde{A}^p_{n_2}\right\}_{\boldsymbol{n}} \sim_\sigma \left(-\widetilde{\mathfrak{a}}_p(\theta_1)\widetilde{\mathfrak{a}}_p(-\theta_2), [-\pi,\pi]^2\right),$$

where

$$\widetilde{\mathfrak{a}}_p(\theta_1)\widetilde{\mathfrak{a}}_p(-\theta_2) = \mathfrak{m}_{p-1}(\theta_1)\mathfrak{m}_{p-1}(\theta_2)(\mathrm{e}^{-\mathbf{i}\theta_1} - 1)(\mathrm{e}^{\mathbf{i}\theta_2} - 1).$$

Now, from the above discussion and from the comments in Subsection 2.4 it is easy to convince that $\widetilde{\mathcal{A}}^{(i,j)}_{\boldsymbol{n}}$, $i,j = 1,2$ is a 2-level Toeplitz matrix up to a low-rank perturbation. More precisely, $\widetilde{\mathcal{A}}^{(i,j)}_{\boldsymbol{n}} = T_{\boldsymbol{n}}(f_{ij}) + E^{(i,j)}_{\boldsymbol{n}}$, $i,j = 1,2$, where $T_{\boldsymbol{n}}(f_{ij})$ is a 2-level Toeplitz matrix generated by $f_{ij} : [-\pi,\pi]^2 \to \mathbb{C}$, $i,j = 1,2$, with

$$\begin{aligned}
f_{11}(\theta_1,\theta_2) &= \frac{\nu_2}{\nu_1}\mathfrak{m}_{p-1}(\theta_1)\mathfrak{m}_{p-1}(\theta_2)(2-2\cos(\theta_2)),\\
f_{12}(\theta_1,\theta_2) &= -\mathfrak{m}_{p-1}(\theta_1)\mathfrak{m}_{p-1}(\theta_2)(\mathrm{e}^{-\mathbf{i}\theta_1}-1)(\mathrm{e}^{\mathbf{i}\theta_2}-1),\\
f_{21}(\theta_1,\theta_2) &= f_{12}(-\theta_1,-\theta_2),\\
f_{22}(\theta_1,\theta_2) &= \frac{\nu_1}{\nu_2}\mathfrak{m}_{p-1}(\theta_1)\mathfrak{m}_{p-1}(\theta_2)(2-2\cos(\theta_1)).
\end{aligned}$$

Furthermore, through a proper permutation matrix Π of size $2\hat{n}$, $\hat{n} = (n_1+p)(n_2+p)$, we can write

$$\Pi\widetilde{\mathcal{A}}_{\boldsymbol{n}}\Pi^T = \Pi\begin{bmatrix} T_{\boldsymbol{n}}(f_{11}) + E^{(1,1)}_{\boldsymbol{n}} & T_{\boldsymbol{n}}(f_{12}) + E^{(1,2)}_{\boldsymbol{n}} \\ T_{\boldsymbol{n}}(f_{21}) + E^{(2,1)}_{\boldsymbol{n}} & T_{\boldsymbol{n}}(f_{22}) + E^{(2,2)}_{\boldsymbol{n}} \end{bmatrix}\Pi^T = T_{\boldsymbol{n}}(f) + E_{\boldsymbol{n}},$$

where $f : [-\pi,\pi]^2 \to \mathbb{C}^{2\times 2}$ is defined as follows:

$$\begin{aligned}
f(\theta_1,\theta_2) &= \begin{bmatrix} f_{11}(\theta_1,\theta_2) & f_{12}(\theta_1,\theta_2) \\ f_{21}(\theta_1,\theta_2) & f_{22}(\theta_1,\theta_2) \end{bmatrix}\\
&= \mathfrak{m}_{p-1}(\theta_1)\mathfrak{m}_{p-1}(\theta_2)\begin{bmatrix} \frac{\nu_2}{\nu_1}(2-2\cos(\theta_2)) & -(\mathrm{e}^{-\mathbf{i}\theta_1}-1)(\mathrm{e}^{\mathbf{i}\theta_2}-1) \\ -(\mathrm{e}^{\mathbf{i}\theta_1}-1)(\mathrm{e}^{-\mathbf{i}\theta_2}-1) & \frac{\nu_1}{\nu_2}(2-2\cos(\theta_1)) \end{bmatrix},
\end{aligned}$$

while $E_{\boldsymbol{n}}$ is a low-rank perturbation whose rank is $o(2\hat{n})$. Therefore, $\Pi\widetilde{\mathcal{A}}_{\boldsymbol{n}}\Pi^T$ is a low-rank perturbation of a 2-level block Toeplitz matrix associated to the 2×2 matrix-valued function f. To write explicitly the permutation matrix Π, let us define by e_j, $j=1,\dots,2\hat{n}$ the jth column of the identity matrix of size $2\hat{n}$ and by π_j, $j=1,\dots,2\hat{n}$ the jth column of Π. Then,

$$\pi_j=\begin{cases} e_{2j-1} & j=1,\dots,\hat{n},\\ e_{2(j-\hat{n})} & j=\hat{n}+1,\dots,2\hat{n}.\end{cases}$$

In other words, Π is the $2\hat{n}\times 2\hat{n}$ matrix whose first $\hat{n}$ columns are the odd columns of the identity matrix of size $2\hat{n}$, while the remaining ones are the even columns of the same matrix.

Note that f is an Hermitian matrix-valued function, then because of Theorem 2.9 (with $d=2$, $s=2$) it holds that $\{T_{\boldsymbol{n}}(f)\}_{\boldsymbol{n}}\sim_\lambda (f,[-\pi,\pi]^2)$. To compute the symbol of $\{\Pi\widetilde{\mathcal{A}}_{\boldsymbol{n}}\Pi^T\}_{\boldsymbol{n}}$, or equivalently of $\{\widetilde{\mathcal{A}}_{\boldsymbol{n}}\}_{\boldsymbol{n}}$, we will use Corollary 3.4 in [11] concerning the spectral distribution of multilevel block Toeplitz sequences plus low-rank perturbations. Without going into details, we only recall that, as stated in Corollary 3.4 in [11], the spectral distribution of a multilevel block Toeplitz sequence is not affected by a low-rank perturbation. On this basis we can conclude that $\{\widetilde{\mathcal{A}}_{\boldsymbol{n}}\}_{\boldsymbol{n}}$ and $\{T_{\boldsymbol{n}}(f)\}_{\boldsymbol{n}}$ have the same spectral distribution, i.e.,

$$\{\widetilde{\mathcal{A}}_{\boldsymbol{n}}\}_{\boldsymbol{n}}\sim_\lambda (f,[-\pi,\pi]^2). \tag{4.14}$$

To retrieve the symbol of the original matrix-sequence $\{\mathcal{A}_{\boldsymbol{n}}\}_{\boldsymbol{n}}$ we show that $\mathcal{A}_{\boldsymbol{n}}$ and $\widetilde{\mathcal{A}}_{\boldsymbol{n}}$ are linked by means of a projection matrix and then use Theorem 4.3.

To write explicitly the projection matrix which links $\mathcal{A}_{\boldsymbol{n}}$ and $\widetilde{\mathcal{A}}_{\boldsymbol{n}}$ let us start observing that

$$A^p_{n_1}=H_1\widetilde{A}^p_{n_1},\qquad A^p_{n_2}=\widetilde{A}^p_{n_2}H_2,$$

where H_1 and H_2 are defined in (4.12) and (4.13), respectively. Therefore,

$$A^p_{n_1}\otimes A^p_{n_2}=(H_1\otimes\widetilde{I}_2)(\widetilde{A}^p_{n_1}\otimes\widetilde{A}^p_{n_2})(\widetilde{I}_1\otimes H_2), \tag{4.15}$$

where $\widetilde{I}_1$, $\widetilde{I}_2$ are the identity matrices of size n_1+p and n_2+p, respectively. Moreover, relations (4.11) imply that

$$\begin{aligned} M^{p-1}_{n_1}\otimes S^p_{n_2}&=(H_1\otimes\widetilde{I}_2)(\widetilde{M}^{p-1}_{n_1}\otimes S^p_{n_2})(H_1^T\otimes\widetilde{I}_2),\\ S^p_{n_1}\otimes M^{p-1}_{n_2}&=(\widetilde{I}_1\otimes H_2^T)(S^p_{n_1}\otimes\widetilde{M}^{p-1}_{n_2})(\widetilde{I}_1\otimes H_2),\end{aligned} \tag{4.16}$$

and hence, putting together equations (4.15) and (4.16), we can write

$$\mathcal{A}_{\boldsymbol{n}}=\mathcal{P}^T_{\boldsymbol{n}}\widetilde{\mathcal{A}}_{\boldsymbol{n}}\mathcal{P}_{\boldsymbol{n}},$$

with

$$\mathcal{P}_{\boldsymbol{n}}=\begin{bmatrix} H_1^T\otimes\widetilde{I}_2 & \mathcal{O}_1\\ \mathcal{O}_2 & \widetilde{I}_1\otimes H_2\end{bmatrix},$$

where $\mathcal{O}_1$ is the identically zero matrix of size $(n_1+p)(n_2+p)\times(n_1+p)(n_2+p-1)$, while $\mathcal{O}_2$ is the identically zero matrix of size $(n_1+p)(n_2+p)\times(n_1+p-1)(n_2+p)$.

Recalling relation (4.14) and applying Theorem 4.3, we can conclude that

$$\{\mathcal{A}_{\boldsymbol{n}}\}_{\boldsymbol{n}}\sim_\lambda (f,[-\pi,\pi]^2).$$

Since f is a two-by-two matrix-valued symbol, we have to study its eigenvalue functions. First of all let us observe that $\det(f(\theta_1,\theta_2))=0$, which means that f is a rank-1 symbol and one of its eigenvalue functions, say $\lambda_1(f(\theta_1,\theta_2))$, is identically

zero. Such a spectral behavior is in line with the theoretical findings on the continuous curl-curl operator which has an infinite dimensional kernel. Because of its rank-1 nature, we can write f as the following dyad:

$$f(\theta_1,\theta_2)=\frac{1}{\nu_1\nu_2}\mathfrak{m}_{p-1}(\theta_1)\mathfrak{m}_{p-1}(\theta_2)\underbrace{\begin{bmatrix}\nu_2(\mathrm{e}^{\mathbf{i}\theta_2}-1)\\ -\nu_1(\mathrm{e}^{\mathbf{i}\theta_1}-1)\end{bmatrix}}_{v(\theta_1,\theta_2)}\underbrace{\begin{bmatrix}\nu_2(\mathrm{e}^{-\mathbf{i}\theta_2}-1) & -\nu_1(\mathrm{e}^{-\mathbf{i}\theta_1}-1)\end{bmatrix}}_{v^H(\theta_1,\theta_2)}.$$

Then we can conclude that the nonidentically zero eigenvalue of $f(\theta_1,\theta_2)$ is the trace of the matrix, that is,

$$\begin{aligned}\lambda_2(f(\theta_1,\theta_2))&=\frac{1}{\nu_1\nu_2}\mathfrak{m}_{p-1}(\theta_1)\mathfrak{m}_{p-1}(\theta_2)\left(v^H(\theta_1,\theta_2)v(\theta_1,\theta_2)\right)\\&=\frac{1}{\nu_1\nu_2}\mathfrak{m}_{p-1}(\theta_1)\mathfrak{m}_{p-1}(\theta_2)\left(\nu_2^2(2-2\cos(\theta_2))+\nu_1^2(2-2\cos(\theta_1))\right).\end{aligned}$$

This second eigenvalue is nothing but the symbol of the Laplacian operator discretized by means of B-splines and as such it has a nice connection with the continuous operator; indeed the curl-curl operator is expected to behave as a second order differential operator on the complement of the kernel. Being f a dyad, we can also easily compute the eigenvectors associated to $\lambda_1(f(\theta_1,\theta_2))$ and $\lambda_2(f(\theta_1,\theta_2))$ as follows:

$$\begin{aligned}z_1(\theta_1,\theta_2)&=\frac{1}{\sqrt{v^H(\theta_1,\theta_2)v(\theta_1,\theta_2)}}\begin{bmatrix}\nu_1(\mathrm{e}^{\mathbf{i}\theta_1}-1)\\ \nu_2(\mathrm{e}^{\mathbf{i}\theta_2}-1)\end{bmatrix},\\ z_2(\theta_1,\theta_2)&=\frac{1}{\sqrt{v^H(\theta_1,\theta_2)v(\theta_1,\theta_2)}}v(\theta_1,\theta_2).\end{aligned}$$

At this point we can compute the symbol of $\{\mathcal{A}_{\boldsymbol{n}}^{\mu}\}_{\boldsymbol{n}}$ as follows:

$$f^{\mu}(\theta_1,\theta_2)=f(\theta_1,\theta_2)+\frac{\mu}{\nu_1\nu_2 n^2}\begin{bmatrix}\mathfrak{m}_{p-1}(\theta_1)\mathfrak{m}_p(\theta_2) & 0\\ 0 & \mathfrak{m}_p(\theta_1)\mathfrak{m}_{p-1}(\theta_2)\end{bmatrix}$$

$$=\frac{1}{\nu_1\nu_2}\mathfrak{m}_{p-1}(\theta_1)\mathfrak{m}_{p-1}(\theta_2)\left(v(\theta_1,\theta_2)v^H(\theta_1,\theta_2)+\frac{\mu}{n^2}D(\theta_1,\theta_2)\right),\tag{4.17}$$

where

$$D(\theta_1,\theta_2)=\begin{bmatrix}\frac{\mathfrak{m}_p(\theta_2)}{\mathfrak{m}_{p-1}(\theta_2)} & 0\\ 0 & \frac{\mathfrak{m}_p(\theta_1)}{\mathfrak{m}_{p-1}(\theta_1)}\end{bmatrix}.$$

Note that according to our notation $f^0\equiv f$. As already observed in [4], the following inequality is satisfied:

$$0<c\le\frac{\mathfrak{m}_p(\theta)}{\mathfrak{m}_{p-1}(\theta)}\le 1,$$

that is, $\frac{\mathfrak{m}_p(\theta)}{\mathfrak{m}_{p-1}(\theta)}$ is a function well-separated from zero, uniformly with respect to $\theta\in[0,\pi]$ and with respect to $p\ge 1$. Applying the well-known min-max theorem,

we obtain

$$\frac{1}{\nu_1\nu_2}\mathfrak{m}_{p-1}(\theta_1)\mathfrak{m}_{p-1}(\theta_2)\frac{\mu}{n^2}c \le \lambda_1\left(f^\mu(\theta_1,\theta_2)\right) \le \frac{1}{\nu_1\nu_2}\mathfrak{m}_{p-1}(\theta_1)\mathfrak{m}_{p-1}(\theta_2)\frac{\mu}{n^2}, \tag{4.18}$$

$$\begin{aligned}\lambda_2\left(f^\mu(\theta_1,\theta_2)\right) &\ge \frac{1}{\nu_1\nu_2}\mathfrak{m}_{p-1}(\theta_1)\mathfrak{m}_{p-1}(\theta_2)\left(\mathcal{L}_{\nu_1,\nu_2}(\theta_1,\theta_2)+\frac{\mu}{n^2}c\right),\\ \lambda_2\left(f^\mu(\theta_1,\theta_2)\right) &\le \frac{1}{\nu_1\nu_2}\mathfrak{m}_{p-1}(\theta_1)\mathfrak{m}_{p-1}(\theta_2)\left(\mathcal{L}_{\nu_1,\nu_2}(\theta_1,\theta_2)+\frac{\mu}{n^2}\right),\end{aligned} \tag{4.19}$$

where

$$\mathcal{L}_{\nu_1,\nu_2}(\theta_1,\theta_2) = v^H(\theta_1,\theta_2)v(\theta_1,\theta_2) = \sum_{j=1}^{2}\nu_j^2(2-2\cos(\theta_j)), \tag{4.20}$$

is exactly the generating function of a pure discrete Laplacian. Indeed, when discretizing $\delta = -\partial_x^2 - \partial_y^2$ over $(0,1)^2$ with Dirichlet boundary conditions, by using the standard Finite Difference five point stencil with $\nu_1 n$ internal points in the x direction and $\nu_2 n$ internal points in the y direction, we end up with the two-level Toeplitz matrix $T_{\boldsymbol{n}}(f)$ where $\boldsymbol{n} = (\nu_1,\nu_2)n$ and $f(\theta_1,\theta_2) \equiv \mathcal{L}_{\nu_1,\nu_2}(\theta_1,\theta_2) = \sum_{j=1}^{2}\nu_j^2(2-2\cos(\theta_j))$, which is the same expression appearing in (4.20).

4.3. **Numerical evidences.** In this subsection we give numerical evidence of the spectral results obtained in the current section. In further detail, we show that the symbol of $\{\mathcal{A}_{\boldsymbol{n}}^\mu\}_{\boldsymbol{n}}$ is $f^\mu(\theta_1,\theta_2)$ defined as in (4.17). Taking into consideration Remark 2.7, this numerical study can be done by comparing the eigenvalues of $\mathcal{A}_{\boldsymbol{n}}^\mu$ with a sampling of the eigenvalue functions $\lambda_1(f^\mu), \lambda_2(f^\mu)$. For our comparisons we use the formal expressions of $\lambda_k(f^\mu)$, $k=1,2$, which are not reported here, since the related formulae do not add much to our findings, neither to the subsequent discussion.

Let us fix $\boldsymbol{n} = (\nu_1 n, \nu_2 n)$, with $\nu_1,\nu_2 = 1$, $n \in \mathbb{N}$ and let us define the following equispaced grid on $[-\pi,\pi]^2$:

$$G_{n,p} = \left\{ (\theta_1^{(j)},\theta_2^{(k)}) = \left(\frac{j\pi}{n+p-1}, \frac{k\pi}{n+p}\right), \begin{array}{l} j=-(n+p-1),\dots,n+p-1 \\ k=-(n+p),\dots,n+p \end{array} \right\}.$$

In Figures 1(A)–1(B) we display the eigenvalue functions $\lambda_k(f^\mu)$, $k=1,2$ on the mesh $G_{n,p}$, fixed $n=40$, $p=3$, $\mu = 10^{-2}$.

From here on, for $k=1,2$, we denote by $\lambda_k(f^\mu)\big|_{G_{n,p}}$ the lexicographically ordered vector of all evaluations of $\lambda_k(f^\mu)$ on $G_{n,p}$, i.e.,

$$\lambda_k(f^\mu)\big|_{G_{n,p}} := \left[\lambda_k(f^\mu(\theta_1^{-(n+p-1)},\theta_2^{-(n+p)})),\dots,\lambda_k(f^\mu(\theta_1^{(n+p-1)},\theta_2^{(n+p)}))\right],$$

and by $\lambda(f^\mu)\big|_{G_{n,p}}$ the vector of all evaluations of $\lambda_k(f^\mu)$ on $G_{n,p}$ varying k, i.e.,

$$\lambda(f^\mu)\big|_{G_{n,p}} := \left[\lambda_1(f^\mu)\big|_{G_{n,p}}, \lambda_2(f^\mu)\big|_{G_{n,p}}\right].$$

As a first evidence that $\{\mathcal{A}_{\boldsymbol{n}}^\mu\}_{\boldsymbol{n}}$ spectrally behaves as $f^\mu(\theta_1,\theta_2)$, in Figure 2 we compare the eigenvalues of $\mathcal{A}_{\boldsymbol{n}}^\mu$ with the evaluations of $\lambda_k(f^\mu)$, $k=1,2$ at $G_{n,p}$ contained in $\lambda(f^\mu)\big|_{G_{n,p}}$ (ordered in ascending way). Here the parameters n,p,μ have been fixed as in Figure 1. Let us observe that, as predicted by the theory, the eigenvalues of $\mathcal{A}_{\boldsymbol{n}}^\mu$ mimic, up to outliers, the considered sampling of $\lambda_k(f^\mu)$, $k=1,2$.

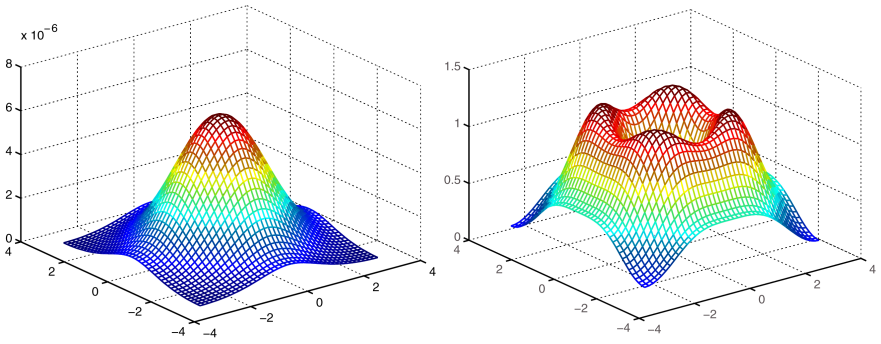

(A) $\lambda_1(f^\mu)$ (B) $\lambda_2(f^\mu)$

FIGURE 1. The eigenvalue functions $\lambda_k(f^\mu)$, $k = 1, 2$ on the mesh $G_{40,3}$, fixed $\mu = 10^{-2}$.

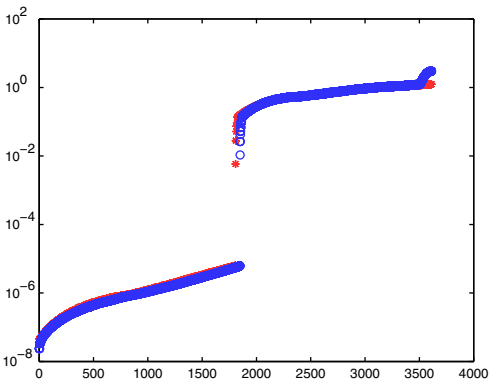

FIGURE 2. Comparison of the eigenvalues of $\mathcal{A}_{\boldsymbol{n}}^{\mu}$ ($\circ$) with $\lambda(f^\mu)\big|_{G_{n,p}}$ ordered in ascending way ($*$), when $n = 40$, $p = 3$, $\mu = 10^{-2}$ (matrix-size 3612).

Aside from such a global comparison, since the following relation holds:

$$\operatorname{esssup}_{[-\pi,\pi]^2}\lambda_1(f^\mu) < \operatorname{essinf}_{[-\pi,\pi]^2}\lambda_2(f^\mu),$$

again according to Remark 2.7, we can provide a more accurate analysis of the spectrum of $\mathcal{A}_{\boldsymbol{n}}^{\mu}$ determining by how many blocks it is made of and how many eigenvalues each block contains. We expect that, up to outliers, a half of the eigenvalues of $\mathcal{A}_{\boldsymbol{n}}^{\mu}$ behaves as $\lambda_1(f^\mu)$ and a half of them behaves as $\lambda_2(f^\mu)$. Furthermore, if we denote by

$$m_k = \min_{G_{n,p}} \lambda_k(f^\mu), \qquad M_k = \max_{G_{n,p}} \lambda_k(f^\mu),$$

we expect the eigenvalues of $\mathcal{A}_{\boldsymbol{n}}^{\mu}$ to identify 2 blocks and to verify

$$\begin{aligned} \#\{i : \lambda_i(\mathcal{A}_{\boldsymbol{n}}^{\mu}) \in [m_1, M_1]\} &= \frac{\dim(\mathcal{A}_{\boldsymbol{n}}^{\mu})}{2} + o(\dim(\mathcal{A}_{\boldsymbol{n}}^{\mu})), \\ \#\{i : \lambda_i(\mathcal{A}_{\boldsymbol{n}}^{\mu}) \in [m_2, M_2]\} &= \frac{\dim(\mathcal{A}_{\boldsymbol{n}}^{\mu})}{2} + o(\dim(\mathcal{A}_{\boldsymbol{n}}^{\mu})), \end{aligned} \tag{4.21}$$

For instance, for n, p, μ as in Figure 1 we have $\dim(\mathcal{A}_{\boldsymbol{n}}^{\mu}) = 3612$, then we expect that approximately 1806 eigenvalues of $\mathcal{A}_{\boldsymbol{n}}^{\mu}$ behave as $\lambda_1(f^{\mu})$ and 1806 eigenvalues behave as $\lambda_2(f^{\mu})$. Indeed, a direct computation shows that

$$\#\{i : \lambda_i(\mathcal{A}_{\boldsymbol{n}}^{\mu}) \in [m_1, M_1]\} = 1828,$$
$$\#\{i : \lambda_i(\mathcal{A}_{\boldsymbol{n}}^{\mu}) \in [m_2, M_2]\} = 1659,$$

and this is in line with the relations in (4.21) since the order of what is missing/exeeding is infinitesimal in the dimension of $\mathcal{A}_{\boldsymbol{n}}^{\mu}$. A confirmation of this behavior can be found in Tables 1 and 2 in which we compare the actual number of eigenvalues of $\mathcal{A}_{\boldsymbol{n}}^{\mu}$ contained in the intervals $[m_1, M_1]$ and $[m_2, M_2]$, respectively, with the expected number $\frac{\dim(\mathcal{A}_{\boldsymbol{n}}^{\mu})}{2}$. In this way, we succeed in counting the outliers of $\mathcal{A}_{\boldsymbol{n}}^{\mu}$ in $[m_1, M_1]$ and $[m_2, M_2]$ and show that their cardinality behaves as $o(\dim(\mathcal{A}_{\boldsymbol{n}}^{\mu}))$.

TABLE 1. Comparison of the effective number of eigenvalues of $\mathcal{A}_{\boldsymbol{n}}^{\mu}$ contained in the interval $[m_1, M_1]$ with the expected number $\dim(\mathcal{A}_{\boldsymbol{n}}^{\mu})/2$.

n	eigs in $[m_1, M_1]$	$\dim(\mathcal{A}_{\boldsymbol{n}}^{\mu})/2$	Out.	Out./$\dim(\mathcal{A}_{\boldsymbol{n}}^{\mu})$
10	160	156	4	0.0128
20	516	506	10	0.0099
30	1072	1056	16	0.0076
40	1828	1806	22	0.0061
50	2780	2756	24	0.0044
60	3936	3906	30	0.0038

TABLE 2. Comparison of the effective number of eigenvalues of $\mathcal{A}_{\boldsymbol{n}}^{\mu}$ contained in the interval $[m_2, M_2]$ with the expected number $\dim(\mathcal{A}_{\boldsymbol{n}}^{\mu})/2$.

n	eigs in $[m_2, M_2]$	$\dim(\mathcal{A}_{\boldsymbol{n}}^{\mu})/2$	Out.	Out./$\dim(\mathcal{A}_{\boldsymbol{n}}^{\mu})$
10	117	156	39	0.1250
20	431	506	75	0.0741
30	945	1056	111	0.0526
40	1659	1806	147	0.0407
50	2572	2756	184	0.0334
60	3687	3906	219	0.0280

Further evidence that $\{\mathcal{A}_{\boldsymbol{n}}^{\mu}\}_{\boldsymbol{n}}$ spectrally behaves as $f^{\mu}(\theta_1, \theta_2)$ can be obtained by comparing the eigenvalues of $\mathcal{A}_{\boldsymbol{n}}^{\mu}$ with the elements of $\lambda(f^{\mu})\big|_{G_{n,p}}$ according to the following matching algorithm:

- for a fixed $\xi \in \Lambda(\mathcal{A}_{\boldsymbol{n}}^{\mu})$ find $\tilde{\eta} \in \lambda(f^{\mu})\big|_{G_{n,p}}$ such that
$$\|\xi - \tilde{\eta}\| = \min_{\eta \in \lambda(f^{\mu})|_{G_{n,p}}} \|\xi - \eta\|,$$
where $\Lambda(\mathcal{A}_{\boldsymbol{n}}^{\mu})$ is the set of all the eigenvalues of $\mathcal{A}_{\boldsymbol{n}}^{\mu}$ and $\|\cdot\|$ is the standard euclidian norm;
- associate ξ to the couple in $G_{n,p}$ corresponding to $\tilde{\eta}$.

Making use of the previous algorithm, in Figure 3 we compare the eigenvalues of $\mathcal{A}_{\boldsymbol{n}}^{\mu}$, $\mu = 10^{-2}$ with $\lambda_k(f^{\mu})$, $k = 1, 2$ displayed as a mesh on $G_{n,p}$, for $n = 40$, $p = 3$. Once again, we can conclude that the eigenvalues of $\mathcal{A}_{\boldsymbol{n}}^{\mu}$ behave, up to few outliers, as a sampling of $\lambda_k(f^{\mu})$, $k = 1, 2$.

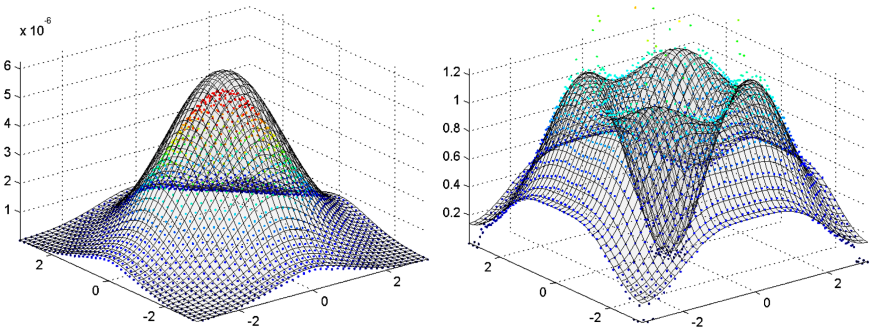

(A) $\lambda_1(f^{\mu})$ (B) $\lambda_2(f^{\mu})$

FIGURE 3. Comparison between the eigenvalues of $\mathcal{A}_{\boldsymbol{n}}^{\mu}$ (colored dots) and $\lambda_k(f^{\mu})$, $k = 1, 2$ displayed as a mesh on $G_{n,p}$ (black surface), when $n = 40$, $p = 3$, $\mu = 10^{-2}$ (matrix-size 3612).

We end this subsection by checking the bounds for the eigenvalue functions $\lambda_k(f^{\mu})$ obtained in (4.18)–(4.19). As shown in Figure 4(A), relation (4.18) holds true on $G_{n,p}$ with parameters p, n, μ fixed as in Figure 1. A confirmation that relation (4.19) holds true as well is given in the small subplot in the lower-right corner of Figure 4(B). We note that in Figure 4(B) only the lower bound is clearly visible because, as expected, the bounds for $\lambda_2(f^{\mu})$ are very sharp.

4.4. **Numerical difficulties when solving large linear systems with IgA curl-curl matrices stabilized with a zero-order term.** In this subsection, in the light of the spectral analysis given so far, we give a concise account of the behavior of classical and more advanced solvers for the solution of the linear systems, whose coefficient matrix is obtained from $\mathcal{A}_{\boldsymbol{n}}^{\mu}$ in (3.7) by imposing the so-called "essential" boundary conditions (see [20] for more details) and by varying the different parameters, $\boldsymbol{n}$, $\boldsymbol{p}$, μ. Below, for simplicity, we refer to this matrix of size $2(n_1+p-1)(n_2+p-2) \times 2(n_1+p-2)(n_2+p-1)$ again as $\mathcal{A}_{\boldsymbol{n}}^{\mu}$ and we fix $\boldsymbol{n} = (n, n)$ and $\boldsymbol{p} = (p, p)$. In detail, we discuss the performances of the conjugate gradient (CG) and of a preconditioner for the CG, whose definition is guided by the knowledge of the symbol of $\{\mathcal{A}_{\boldsymbol{n}}^{\mu}\}_{\boldsymbol{n}}$ and is given by

(4.22)
$$P_{\boldsymbol{n}}^{[\boldsymbol{p}]} = \begin{bmatrix} T_{n+p-1}(\mathfrak{m}_{p-1}(\theta_1)) \otimes T_{n+p-2}(\mathfrak{m}_{p-1}(\theta_2)) & \mathbf{0} \\ \mathbf{0} & T_{n+p-2}(\mathfrak{m}_{p-1}(\theta_1)) \otimes T_{n+p-1}(\mathfrak{m}_{p-1}(\theta_2)) \end{bmatrix}.$$

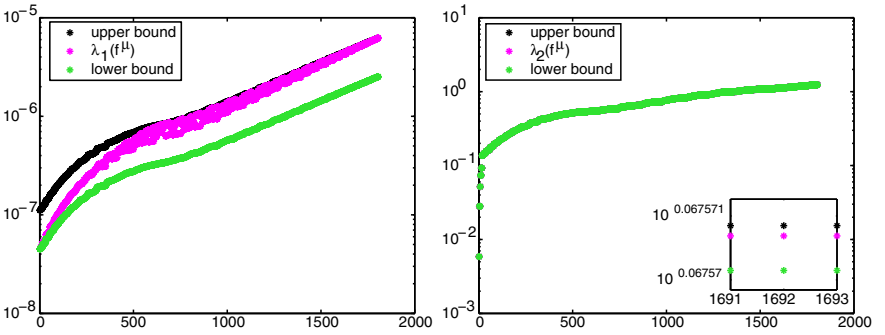

(A) bounds for $\lambda_1(f^\mu)$ (B) bounds for $\lambda_2(f^\mu)$

FIGURE 4. Check of the lower bounds and upper bounds in (4.18)–(4.19) for the eigenvalue functions $\lambda_k(f^\mu)$, $k = 1, 2$ on $G_{n,p}$, when $n = 40$, $p = 3$, $\mu = 10^{-2}$.

In other words, $P_{\boldsymbol{n}}^{[\boldsymbol{p}]}$ is a direct sum of two 2-level Toeplitz matrices generated by $\mathfrak{m}_{p-1}(\theta_1)\mathfrak{m}_{p-1}(\theta_2)$. Recalling the expression of $f^\mu(\theta_1, \theta_2)$ in (4.17) and the bounds in (4.18)–(4.19), it turns out that, when $\mu > 0$, the following function

$$\mathfrak{m}_{p-1}^{-1}(\theta_1)\mathfrak{m}_{p-1}^{-1}(\theta_2)\lambda_j(f^\mu(\theta_1, \theta_2)), \quad j = 1, 2,$$

is positive and independent of p, then we expect that using $P_{\boldsymbol{n}}^{[\boldsymbol{p}]}$ as a preconditioner for the CG will result in a more robust solver with respect to the degree p. Note that such a preconditioner is easy to construct since we have

$$(T_m(\mathfrak{m}_{p-1}(\theta_k))_{i,j} = \begin{cases} \phi_{2p-1}(p-i+j), & \text{if } |i-j| < p, \\ 0, & \text{otherwise,} \end{cases}$$

i.e., its entries are nothing but evaluations of cardinal B-splines. Moreover, due to its tensor product nature, the linear system whose coefficient matrix is the preconditioner (4.22) is easily solvable and computationally cheap. Indeed, by the properties of Kronecker product we obtain

$$(P_{\boldsymbol{n}}^{[\boldsymbol{p}]})^{-1} = \begin{bmatrix} T_{n+p-1}^{-1}(\mathfrak{m}_{p-1}(\theta_1))\otimes T_{n+p-2}^{-1}(\mathfrak{m}_{p-1}(\theta_2)) & \mathbf{0} \\ \mathbf{0} & T_{n+p-2}^{-1}(\mathfrak{m}_{p-1}(\theta_1))\otimes T_{n+p-1}^{-1}(\mathfrak{m}_{p-1}(\theta_2)) \end{bmatrix}.$$

The linear systems related to the diagonal blocks of $(P_{\boldsymbol{n}}^{[\boldsymbol{p}]})^{-1}$ can be solved by means of an LU factorization which is optimal for banded matrices, i.e., linear in the matrix-size (and quadratic in the bandwidth). Therefore, the computational cost for solving a linear system with coefficient matrix (4.22) is linear in the matrix-size $2(n+p-1)(n+p-2)$.

Regarding the stopping criterion for the CG, we use $\|r^k\|_2/\|r^0\|_2 < 10^{-7}$, where r^k is the residual vector after k iterations. The initial guess is always chosen as the zero vector. For our test examples, we choose the vector solution $\tilde{\boldsymbol{u}}$ as an equispaced sampling of the function

$$\varphi(x_1, x_2) = \sin(3x_1) + \sin(3x_2), \qquad (x_1, x_2) \in (0, \pi)^2,$$

and as the right-hand side $\boldsymbol{b} = \mathcal{A}_{\boldsymbol{n}}^{\mu}\tilde{\boldsymbol{u}}$. Moreover, we test the considered methods both in terms of iterations and of relative approximation error defined as

$$\text{Error} = \frac{\|\boldsymbol{u} - \tilde{\boldsymbol{u}}\|_2}{\|\tilde{\boldsymbol{u}}\|_2},$$

where $\boldsymbol{u}$ is the numerical solution.

When $\mu = 0$, as computed in Subsection 4.2, the number of eigenvalues of $\mathcal{A}_{\boldsymbol{n}}$ in a neighborhood of zero is given by $\frac{\dim(\mathcal{A}_{\boldsymbol{n}})}{2} + o(\dim(\mathcal{A}_{\boldsymbol{n}}))$ and their values are very close to zero independently of the matrix size (see Table 3). Therefore the considered matrices can be viewed as the discretization of an ill-posed problem [6].

TABLE 3. Number of eigenvalues smaller than a fixed threshold in the set $\{10^{-2}, 10^{-4}, 10^{-8}\}$ and minimum eigenvalue of $\mathcal{A}_{\boldsymbol{n}}^{\mu}$ when $\mu = 0$, $p = 3$, and varying n.

n	$\dim(\mathcal{A}_{\boldsymbol{n}}^{\mu})$	eigs $< 10^{-2}$	eigs $< 10^{-4}$	eigs $< 10^{-8}$	min eig
4	60	25	25	25	-0.0478e-14
8	180	81	81	81	-0.0941e-14
16	612	289	289	289	-0.1402e-14
32	2244	1091	1089	1089	-0.2129e-14
64	8580	4230	4225	4225	-0.4394e-14

TABLE 4. CG iterations and approximation error when $p = 3$, $\mu = 10^{-2}$, $n = 8, 16, 32, 64, 128$.

n	CG Iter	Error
8	161	9.698e-003
16	237	1.490e-002
32	246	2.758e-002
64	314	3.723e-002
128	528	3.436e-002

TABLE 5. CG iterations and approximation error when $p = 3$, $n = 64$, $\mu = 1, 10^{-1}, 10^{-2}, 10^{-3}, 10^{-4}$.

μ	CG Iter	Error
1	750	2.053e-003
10^{-1}	545	9.565e-003
10^{-2}	314	3.723e-002
10^{-3}	156	3.202e-001
10^{-4}	106	5.491e-001

Hence, as in a standard Tikhonov for image deblurring and denoising [6], we need a kind of regularization and this is done by using the parameter $\mu > 0$. In any case $\mu > 0$ has to be chosen small and therefore also the matrices $\mathcal{A}_{\boldsymbol{n}}^{\mu}$ are very ill-conditioned and possess $\frac{\dim(\mathcal{A}_{\boldsymbol{n}}^{\mu})}{2} + o(\dim(\mathcal{A}_{\boldsymbol{n}}^{\mu}))$ eigenvalues in a neighborhood of the interval (m_1, M_1), with both m_1 and M_1 converging linearly to zero as μ goes to zero (see (4.18) and the numerical experiments in Subsection 4.3). The latter choice has two consequences:

- if we fix $\mu > 0$, but "small", then the CG method is slow and this slow behavior is due to a subspace of large dimension. As a result, we see a significant growth of the iteration number with n (refer to Table 4);
- if we fix the size n, then we see a deterioration of the error as μ becomes smaller and the number of iterations is no more reliable (refer to Table 5).

However, even when we fix the size n and we take $\mu > 0$ not so "small", there is a third source of ill-conditioning hidden in the degree p of the B-spline. Such a behavior is confirmed in Table 6 for $\mu = 10^{-1}$ and $n = 64$. On the other hand, as shown in the same table, using $P_{\boldsymbol{n}}^{[\boldsymbol{p}]}$ as preconditioner the number of iterations of the CG reveals less sensible with respect to the degree p.

TABLE 6. Comparison between the iteration number and the approximation error provided by the unprecoditioned CG and the CG preconditioned with $P_{\boldsymbol{n}}^{[\boldsymbol{p}]}$ (PCG) when $\mu = 10^{-1}$, $n = 64$, $p = 1, \ldots, 5$.

p	$\dim(\mathcal{A}_{\boldsymbol{n}}^{\mu})$	CG Iter	Error	PCG Iter	Error
1	8064	331	3.022e-003	331	3.022e-003
2	8320	348	7.877e-003	427	7.280e-003
3	8580	545	9.565e-003	495	8.695e-003
4	8844	1001	1.559e-002	553	9.437e-003
5	9112	1939	2.891e-002	594	1.942e-002

These numerical results can be spectrally justified as follows. As for the symbol of the IgA stiffness matrix-sequence (recall Remark 2.14), it can be shown that the eigenvalue functions $\lambda_j(f^{\mu}(\theta_1, \theta_2))$, $j = 1, 2$, satisfy the following properties:

(i) for $\mu = 0$ $\lambda_2(f^{\mu}(\theta_1, \theta_2))$ has an analytic zero in $(\theta_1, \theta_2) = (0, 0)$ of order 2, $\lambda_1(f^{\mu}(\theta_1, \theta_2))$ is identically zero;
(ii) both $\lambda_1(f^{\mu}(\theta_1, \theta_2))$ and $\lambda_2(f^{\mu}(\theta_1, \theta_2))$ possess infinitely many numerical exponential zeros at the points (θ_1, θ_2) with $\theta_j = \pi$ when p becomes large.

For fixed small μ, properties (i)–(ii) imply that the small eigenvalues of $\mathcal{A}_{\boldsymbol{n}}^{\mu}$ are related both with subspaces of low and high frequencies. As confirmed by the slowing down of the iteration number as p increases, the preconditioner $P_{\boldsymbol{n}}^{[\boldsymbol{p}]}$ is acting in the high frequencies. In [4] a robust and optimal technique for dealing, simultaneously, with the combination of low-frequency/high-frequency ill-conditioning has been proposed. Such a technique is of multi-iterative type [21] and is obtained by combining a multigrid method able to cut the ill-conditioning in the low-frequencies with a preconditioning acting in the high frequencies, in the same spirit of preconditioner $P_{\boldsymbol{n}}^{[\boldsymbol{p}]}$. Unfortunately, the same technique suffers a lot from the source of ill-conditioning due by the fact that, even when $\mu > 0$, one half of the eigenvalues of $\mathcal{A}_{\boldsymbol{n}}^{\mu}$ are uniformly small. In the next subsection, we show how an ad hoc stabilization term can reduce this kind of ill-conditioning and, as a consequence, how a vector extension of the method proposed in [4] becomes efficient also for our problem.

4.5. **Numerical results when solving large linear systems with IgA curl-curl matrices stabilized with a divergence-type term.** As we have already mentioned in the previous subsection the spectral analysis performed in Subsection 4.2 gives a strong information on the difficulty related to the solution of the linear systems associated to $\mathcal{A}_{\boldsymbol{n}}^{\mu}$: we have 3 separated sources of ill-conditioning, the one induced by the fact that the symbol without stabilization is a dyad, the one in low-frequency induced by the nonzero Laplacian-like eigenvalue of the symbol, the one in high-frequency induced by the parameter p of the B-spline approximation [4, 7].

The unsatisfactory performances of both classical methods, like CG method, and of more advanced solvers, like the one in [4], when solving linear systems associated to $\mathcal{A}_{\boldsymbol{n}}^{\mu}$ suggest to adopt another stabilization term. Indeed, if we replace the zero-order term with a divergence-like one, then a Laplacian will be present both in the problem (the nontrivial eigenvalue of the symbol without stabilization) and in the stabilization. The latter modification will make the stabilized problem somehow spectrally similar to the problem treated in [4]. As a consequence, we expect that a vector extension of the method proposed therein will work much more satisfactorily for the new stabilized problem as well. On the other hand, we have to stress that the new stabilization can be taken at the prize of giving up the properties of the compatible spaces and of the de Rham sequence.

Formally, the discrete variational problem (3.1) becomes

$$\boldsymbol{u} \in \boldsymbol{V}_h(\mathrm{grad}, \Omega): \quad (\nabla \times \boldsymbol{u}, \nabla \times \boldsymbol{v}) + \mu\,(\nabla \cdot \boldsymbol{u}, \nabla \cdot \boldsymbol{v}) = (\boldsymbol{f}, \boldsymbol{v}) \quad \forall \boldsymbol{v} \in \boldsymbol{V}_h(\mathrm{grad}, \Omega),$$

with $\boldsymbol{V}_h(\mathrm{grad}, \Omega) = \left(\begin{smallmatrix} S^{p,p} \\ S^{p,p} \end{smallmatrix}\right)$ and $\Omega = [0,1]^2$. The corresponding coefficient matrix is

$$\mathcal{B}_{\boldsymbol{n}}^{\mu} = \begin{bmatrix} M_{n_1}^p \otimes S_{n_2}^p & -(A_{n_1}^p)^T \otimes A_{n_2}^p \\ -A_{n_1}^p \otimes (A_{n_2}^p)^T & S_{n_1}^p \otimes M_{n_2}^p \end{bmatrix} + \mu \begin{bmatrix} S_{n_1}^p \otimes M_{n_2}^p & A_{n_1}^p \otimes (A_{n_2}^p)^T \\ (A_{n_1}^p)^T \otimes A_{n_2}^p & M_{n_1}^p \otimes S_{n_2}^p \end{bmatrix}$$

with M_n^p, S_n^p as in (2.8)–(2.9) and $A_n^p = \int_0^1 N_i^p(t)(N_j^p(t))'\,dt$. In Tables 7 and 8 we test the effectiveness of the following multi-iterative scheme:

- a V-cycle with two-by-two block bilinear interpolation prolongation operator at each level (number of recursion levels given by $s = \log_2(n + p - 1)$);
- one Gauss-Seidel pre-smoothing iteration at each level;
- p post-smoothing iterations of PGMRES at the finest level whose preconditioner is chosen as $P_{\boldsymbol{n}}^{[\boldsymbol{p}]}$ and one Gauss-Seidel post-smoothing iteration at the other levels.

We use this method for solving the linear system associated to $\mathcal{B}_{\boldsymbol{n}}^{\mu}$ with homogeneous boundary conditions: we refer to it as "MIM" when applied as a stand alone method or as "P_{MIM}" when used as preconditioner for the CG method. More precisely, Tables 7 and 8 refer to the comparison in terms of iterations of both MIM and P_{MIM} with the CG method, by taking the same test example as in Subsection 4.4. Note that in all tables we choose n in order to maintain the same matrix-size for each p.

As shown in Table 7, for $\mu = 10^{-1}$ both P_{MIM} and MIM are optimal and robust with respect to n and p, while the number of iterations of the CG increases in the matrix-size and in the degree as well. A similar behavior is obtained when we decrease μ to 10^{-2} (see Table 8). However, now P_{MIM} outperforms both MIM and the CG. The latter means that the strategy of using the multi-iterative method as

preconditioner succeeds in guaranteeing robustness with respect to n and p and to obtaining an acceptable dependency on the stabilization parameter μ.

A detailed spectral study of the matrix-sequence $\{\mathcal{B}^{\mu}_{\boldsymbol{n}}\}_{\boldsymbol{n}}$ and a deeper theoretical explanation of all the obtained numerical results will be subject of further research.

TABLE 7. Number of iterations provided by P_{MIM}, MIM, and by the CG method when $\mu = 10^{-1}$

$p=1$				$p=2$				$p=3$			
n	P_{MIM}	MIM	CG	n	P_{MIM}	MIM	CG	n	P_{MIM}	MIM	CG
16	6	18	76	15	5	12	49	14	4	10	52
32	6	17	149	31	5	11	94	30	5	10	94
64	6	16	280	63	5	11	180	62	5	10	187
$p=4$				$p=5$				$p=6$			
n	P_{MIM}	MIM	CG	n	P_{MIM}	MIM	CG	n	P_{MIM}	MIM	CG
13	4	10	105	12	5	11	206	11	6	13	330
29	4	10	119	28	5	11	231	27	6	13	475
61	5	10	192	60	5	11	265	59	5	13	522

TABLE 8. Number of iterations provided by P_{MIM}, MIM, and by the CG method when $\mu = 10^{-2}$

$p=1$				$p=2$				$p=3$			
n	P_{MIM}	MIM	CG	n	P_{MIM}	MIM	CG	n	P_{MIM}	MIM	CG
16	16	105	166	15	15	94	128	14	13	77	124
32	17	115	352	31	15	83	237	30	14	73	234
64	17	118	698	63	14	72	449	62	14	68	460
$p=4$				$p=5$				$p=6$			
n	P_{MIM}	MIM	CG	n	P_{MIM}	MIM	CG	n	P_{MIM}	MIM	CG
13	13	67	149	12	14	70	273	11	16	78	464
29	13	65	240	28	13	60	330	27	14	66	602
61	13	65	476	60	13	62	510	59	13	60	667

5. Conclusions and future works

We have studied structural and spectral features of linear systems of equations arising from Galerkin approximations of $H(\mathrm{curl})$ elliptic variational problems, based

on the Isogeometric approach. First, we considered a compatible B-splines discretization based on a discrete de Rham sequence and we identified the structure of the resulting matrix $\mathcal{A}_{\boldsymbol{n}}$, which shows a two-by-two pattern and is a principal submatrix of a two-by-two block matrix, where each block is two-level banded, almost Toeplitz, and where the bandwidths grow linearly with the degree of the B-splines.

Looking at the coefficients in detail and making use of the theory of the GLT sequences, we computed the symbol of each of these blocks, that is, a function describing asymptotically, i.e., for $\boldsymbol{n}$ large enough, the spectrum of each block. From this knowledge and thanks to some new spectral tools we recovered the symbol of $\{\mathcal{A}_{\boldsymbol{n}}\}_{\boldsymbol{n}}$ which as expected is a two-by-two matrix-valued bivariate trigonometric polynomial. In particular, there is a nice elegant connection with the continuous operator which has an infinite dimensional kernel, and in fact the symbol is a dyad having one eigenvalue like the one of the IgA Laplacian, and one identically zero eigenvalue: as a consequence, we proved that one half of the spectrum of $\mathcal{A}_{\boldsymbol{n}}$, for $\boldsymbol{n}$ large enough, is very close to zero and this represents the discrete counterpart of the infinite dimensional kernel of the continuous operator. From the latter information, we gave a detailed spectral analysis of the matrices $\mathcal{A}_{\boldsymbol{n}}$ and of their stabilized versions $\mathcal{A}^{\mu}_{\boldsymbol{n}}$, which is fully confirmed by several numerical evidences.

Finally, by taking into consideration the GLT theory and making use of the spectral results, we furnished indications on the convergence features of known iterative solvers and we suggested a further stabilization technique and proper iterative procedures for the numerical solution of the involved linear systems.

The spectral analysis presented in this paper will provide a strong guidance for the forthcoming works. On the one hand we will perform a more detailed study of the multi-iterative approach discussed at the end of Subsection 4.5 as a way to overcome the ill-conditioning related to the matrix-size and the degree of the B-splines. On the other hand, we will face the ill-conditioning related to the stabilization parameter using some sort of splitting strategy able to isolate the huge kernel of the curl-curl operator from its orthogonal where the operator behaves like a second order operator. In this direction we will extend also in the IgA framework the so-called auxiliary space preconditioning (introduced for Finite Elements in [14]) whose main idea consists of transferring the original problem to one or more simpler spaces (called auxiliary spaces) where the problem can be solved in an easier way, and then to transfer back the solution correcting the mismatch between the original space and the auxiliary spaces with some smoothing scheme.

References

[1] R. Bhatia, *Matrix Analysis*, Graduate Texts in Mathematics, vol. 169, Springer-Verlag, New York, 1997. MR1477662

[2] A. Buffa, G. Sangalli, and R. Vázquez, *Isogeometric analysis in electromagnetics: B-splines approximation*, Comput. Methods Appl. Mech. Engrg. **199** (2010), no. 17-20, 1143–1152, DOI 10.1016/j.cma.2009.12.002. MR2594830

[3] L. Chacón, *An optimal, parallel, fully implicit Newton-Krylov solver for three-dimensional viscoresistive magnetohydrodynamics*, Phys. Plasmas **15** (2008), no. 5, 056103.

[4] M. Donatelli, C. Garoni, C. Manni, S. Serra-Capizzano, and H. Speleers, *Robust and optimal multi-iterative techniques for IgA Galerkin linear systems*, Comput. Methods Appl. Mech. Engrg. **284** (2015), 230–264, DOI 10.1016/j.cma.2014.06.001. MR3310285

[5] M. Donatelli, C. Garoni, C. Manni, S. Serra-Capizzano, and H. Speleers, *Symbol-based multigrid methods for Galerkin B-spline isogeometric analysis*, SIAM J. Numer. Anal. **55** (2017), no. 1, 31–62, DOI 10.1137/140988590. MR3592079

[6] H. W. Engl, M. Hanke, and A. Neubauer, *Regularization of Inverse Problems*, Mathematics and its Applications, vol. 375, Kluwer Academic Publishers Group, Dordrecht, 1996. MR1408680

[7] C. Garoni, C. Manni, F. Pelosi, S. Serra-Capizzano, and H. Speleers, *On the spectrum of stiffness matrices arising from isogeometric analysis*, Numer. Math. **127** (2014), no. 4, 751–799, DOI 10.1007/s00211-013-0600-2. MR3229992

[8] C. Garoni and S. Serra-Capizzano, *Generalized locally Toeplitz Sequences: Theory and Applications. Vol. I*, Springer, Cham, 2017. MR3674485

[9] C. Garoni and S. Serra-Capizzano, *The Theory of Multilevel Generalized Locally Toeplitz Sequences: Theory and Applications - Vol II*, Springer Monographs, 2017, in preparation. Preliminary version in: Technical Report, N. 2, February 2017, Department of Information Technology, Uppsala University.

[10] C. Garoni, S. Serra-Capizzano, and D. Sesana, *Spectral analysis and spectral symbol of d-variate $\mathbb{Q}_p$ Lagrangian FEM stiffness matrices*, SIAM J. Matrix Anal. Appl. **36** (2015), no. 3, 1100–1128, DOI 10.1137/140976480. MR3376130

[11] C. Garoni, S. Serra-Capizzano, and D. Sesana, *Tools for determining the asymptotic spectral distribution of non-Hermitian perturbations of Hermitian matrix-sequences and applications*, Integral Equations Operator Theory **81** (2015), no. 2, 213–225, DOI 10.1007/s00020-014-2157-6. MR3299836

[12] L. Golinskii and S. Serra-Capizzano, *The asymptotic properties of the spectrum of nonsymmetrically perturbed Jacobi matrix sequences*, J. Approx. Theory **144** (2007), no. 1, 84–102, DOI 10.1016/j.jat.2006.05.002. MR2287378

[13] U. Grenander and G. Szegő, *Toeplitz Forms and their Applications*, 2nd ed., Chelsea Publishing Co., New York, 1984. MR890515

[14] R. Hiptmair and J. Xu, *Nodal auxiliary space preconditioning in* $\mathbf{H}(\mathbf{curl})$ *and* $\mathbf{H}(\mathrm{div})$ *spaces*, SIAM J. Numer. Anal. **45** (2007), no. 6, 2483–2509, DOI 10.1137/060660588. MR2361899

[15] R. Hiptmair and W. Zheng, *Local multigrid in* $\mathbf{H}(\mathbf{curl})$, J. Comput. Math. **27** (2009), no. 5, 573–603, DOI 10.4208/jcm.2009.27.5.012. MR2536903

[16] T. J. R. Hughes, J. A. Cottrell, and Y. Bazilevs, *Isogeometric analysis: CAD, finite elements, NURBS, exact geometry and mesh refinement*, Comput. Methods Appl. Mech. Engrg. **194** (2005), no. 39-41, 4135–4195, DOI 10.1016/j.cma.2004.10.008. MR2152382

[17] T. V. Kolev and P. S. Vassilevski, *Auxiliary space AMG for H(curl) problems*, Domain decomposition methods in science and engineering XVII, Lect. Notes Comput. Sci. Eng., vol. 60, Springer, Berlin, 2008, pp. 147–154, DOI 10.1007/978-3-540-75199-1_13. MR2436078

[18] T. V. Kolev and P. S. Vassilevski, *Parallel auxiliary space AMG for H(curl) problems*, J. Comput. Math. (2009), 604–623.

[19] M. Mazza, C. Manni, A. Ratnani, S. Serra-Capizzano, and H. Speleers, *Isogeometric analysis for 2D and 3D curl-div problems: Spectral symbols and fast iterative solvers*, ArXiv:1805.10058, 2018.

[20] P. Monk, *Finite Element Methods for Maxwell's Equations*, Numerical Mathematics and Scientific Computation, Oxford University Press, New York, 2003. MR2059447

[21] S. Serra, *Multi-iterative methods*, Comput. Math. Appl. **26** (1993), no. 4, 65–87, DOI 10.1016/0898-1221(93)90035-T. MR1223858

[22] S. Serra Capizzano, *An ergodic theorem for classes of preconditioned matrices*, Linear Algebra Appl. **282** (1998), no. 1-3, 161–183, DOI 10.1016/S0024-3795(98)80002-5. MR1648324

[23] S. Serra Capizzano, *Test functions, growth conditions and Toeplitz matrices*, Proceedings of the Fourth International Conference on Functional Analysis and Approximation Theory, Vol. II (Potenza, 2000), Rend. Circ. Mat. Palermo (2) Suppl. **68** (2002), 791–795. MR1975486

[24] S. Serra Capizzano, *Generalized locally Toeplitz sequences: spectral analysis and applications to discretized partial differential equations*, Linear Algebra Appl. **366** (2003), 371–402, DOI 10.1016/S0024-3795(02)00504-9. Special issue on structured matrices: analysis, algorithms and applications (Cortona, 2000). MR1987730

[25] S. Serra-Capizzano, *The GLT class as a generalized Fourier analysis and applications*, Linear Algebra Appl. **419** (2006), no. 1, 180–233, DOI 10.1016/j.laa.2006.04.012. MR2263117

[26] P. Tilli, *Locally Toeplitz sequences: spectral properties and applications*, Linear Algebra Appl. **278** (1998), no. 1-3, 91–120, DOI 10.1016/S0024-3795(97)10079-9. MR1637331

[27] P. Tilli, *A note on the spectral distribution of Toeplitz matrices*, Linear and Multilinear Algebra **45** (1998), no. 2-3, 147–159, DOI 10.1080/03081089808818584. MR1671591

Max-Planck Institut für Plasmaphysik, Boltzmannstrasse 2, 87548 Garching bei, München, Germany

Email address: mariarosa.mazza@ipp.mpg.de

Max-Planck Institut für Plasmaphysik, Boltzmannstrasse 2, 87548 Garching bei, München, Germany; and Technische Universität München, Boltzmannstrasse 3, 87548 Garching bei München, Germany

Email address: ahmed.ratnani@ipp.mpg.de

Department of Science and High Technology, University of Insubria, Via Valleggio 11, 22100 Como, Italy; and Department of Information Technology, Uppsala University, Box 337, SE-751 05 Uppsala, Sweden

Email address: stefano.serrac@uninsubria.it